2013

# Fault Location in Power Networks Using Synchronized Phasor Measurements

Cuong Nguyen
*University of South Carolina*

# FAULT LOCATION IN POWER NETWORKS USING SYNCHRONIZED PHASOR MEASUREMENTS

by

Cuong Nguyen

Bachelor of Science
Hanoi University of Science and Technology, 2009

---

Submitted in Partial Fulfillment of the Requirements

For the Degree of Master of Science in

Electrical Engineering

College of Engineering and Computing

University of South Carolina

2013

Accepted by:

Charles Brice, Director of Thesis

Enrico Santi, Reader

Lacy Ford, Vice Provost and Dean of Graduate Studies

# ACKNOWLEDGEMENTS

I would like to express my deepest appreciation to my advisor, Dr. Charles Brice. Without his guidance and support, my graduate studies at University of South Carolina would not have been completed. I would like to thank Dr. Enrico Santi for serving as my thesis committee member and for the knowledge he provided during his classes and during my thesis preparation. I would also like to thank Dr. Yong-June Shin for his support throughout the course of my studies.

I would like express my gratitude to my fellow graduate students and friends in Power and Energy group. Much appreciation also goes go to faculty and staff members at Department of Electrical Engineering, University of South Carolina.

Finally, I would like to thank my parents and my brother whose love, support and encouragement have made this journey possible.

# ABSTRACT

Faults in electric power systems can lead to cascading power outages which cause tremendous loss to the economy and affect people's lives. Technical reports of recent blackout events in the United States pointed out the lack of situational awareness as one of the main causes of widespread outages. Time synchronized phasor measurement is recommended as a technology that can improve the monitoring of power system condition. By knowing exactly where a fault occurs, necessary actions can be taken in a timely manner and thus, damage caused by that fault can be limited. In this thesis, first, a method for precise frequency and phasor measurement is proposed. This novel method bases on the linear combination of selected Discrete Fourier Transform terms and is able to eliminate estimation error at off-nominal frequency. Second, the thesis presents a method to locate fault in power network using voltage and current phasor measurements. This fault location method involves the calculation of impedance matrix when network topology changes during fault and fault location is found by matching the calculated values of voltage and current phasors with its real world measurements. The proposed method is implemented in MATLAB and is demonstrated in three example networks simulated in PSCAD.

# TABLE OF CONTENTS

# LIST OF TABLES

# LIST OF FIGURES

# CHAPTER 1

## INTRODUCTION

Electric power systems have been changing to meet the growing need of electricity. The growth of electric energy consumption in the United States is 2.1% per year from 1980 to 2000 [4].While the energy demand is increasing, the transmission systems is stressed harder since adding new transmission lines is difficult. Legal issue, concern about environmental impact, land availability and others make the expansion of transmission network a complicated process. At the same time, the aging of grid infrastructure increases the system's vulnerability to failure. Strengthening the U.S. grid is now an urgent need as its failure can cause tremendous loss to the economy and affect people life. The Northeast blackout of 2003 affected approximately 50 million people, caused disruption in power generation, water supply, transportation, communication and other industries. The cascading outage was initiated in Ohio amid high electrical demand. Investigation stated that a transmission line went out of service due to tree contact and highlighted the inadequate situational awareness as one of the causes lead to the blackout [1].

The spread of cascading outage in future can be limited by correcting its direct causes: the lack of situational awareness. Technical analysis of the Northeast blackout of 2013 by North American Electric Reliability Council recommended installing additional time-synchronized data recording devices, such as phasor measurement units, to improve the

monitoring of power system condition. As the number of phasor measurement units deployed is increasing, numerous algorithms have been proposed to utilize the information obtained. Synchrophasor measurements can be used in applications such as state estimation, disturbance monitoring, post disturbance analysis, adaptive protection, real time automated grid control, etc. [5].

Dealing with fault in transmission and distribution lines is always a part of power system's operation. Faults are caused by many reasons such as lightning, rain, short circuit caused by insulation break down, tree touching, etc. When a fault occurs, protection devices will response to the disturbance created by that fault and faulted line may be taken out of service. Protection devices are coordinated in the way that provides maximum sensitivity to fault and undesirable conditions but their operation on permissible conditions have to be avoided, as mentioned by Blackburn in [6]. A fault locator that provides the exact location of fault can enhance the operation of protection system. Series circuit breaker trips that lead to blackout in large area can be prevented if fault location is identified quickly. For long transmission lines, fault locator can reduce the labor required for maintenance and restore the service quicker since patrol is not needed. An effective fault locator can help minimize the damage caused by a fault and improve the quality of service for the customer.

Performance of fault location devices currently used in power system can be enhanced with the new data provided by phasor measurement units. In this thesis, chapter 2 and chapter 3 will discuss synchrophasor measurements and chapter 4 and chapter 5 focus on the using of synchrophasor measurements to find fault location. Chapter 2 of this thesis is the fundamental of time synchronized phasor. Basic configuration of a phasor

measurement unit and its phasor and frequency estimation algorithms is discussed. The presented estimation algorithms are based on calculation of Discrete Fourier Transform term at fundamental frequency. In chapter 3, limitation of the classical frequency estimation method is analyzed. Mathematic derivation of Discrete Fourier Transform explains the error of classical method for input signal at off-nominal frequency. Base on the analysis, a novel frequency estimation method using linear combination of Discrete Fourier Transform terms at selected frequencies is proposed. The idea of this method is to calculate the coefficients of the linear combination in order to reduce the error caused when input signal's frequency is not nominal. Chapter 4 discusses the issue of fault location in power systems. First, an overview of fundamental fault location techniques is provided. Then, we present the method to locate fault at power network level using voltage and current phasor measurements. The principle of this method is to match the calculated values of voltage and currents at certain buses and lines with the real world measurements of these voltages and currents. This fault location method involves the calculation of impedance matrix when network topology changes and matching problem is solved by non-linear least squares. This method is applied to three example cases in chapter 5. The three example cases are 6 bus system, single circuit line and double circuit lines. The proposed algorithms are tested using PSCAD simulations. This chapter also presents the calculation of equivalent model for the case of single circuit line and double circuit lines from current and voltage phasor measurements.

# CHAPTER 2

## TIME SYNCHRONIZED PHASOR MEASUREMENTS

Voltage and current phasor information are important to power system monitoring and control. A change in magnitude or phase angle can indicate a fault on transmission line, generator loss, load change, etc. However, as measurements in power systems are transmitted to operation centers from various locations across a large geographical area, the report delay caused by communication decrease the accuracy of obtained information. Using voltage and current phasors without knowing exactly the moment it is measured can lead to the wrong interpretation of the data and it can diminish the ability to take control action when an event happens. Fortunately, with the development of Global Positioning System (GPS), high performance micro-processor and high bandwidth communication, the phasor and other information can be synchronized with the accurate time frame and transmitted to across the long distance. Phasor measurement unit (PMU) was invented in 1988 by A.G. Phadke and J.S. Thorp at Virginia Tech. The device measures real-time phasors of electrical waveforms in power systems using a common time source (GPS) for synchronization [15]. In this chapter, PMU and its applications will be briefly discussed. Following it is the basic algorithms for phasor and frequency estimation used in PMU.

## 2.1. PHASOR MEASUREMENT UNIT

Figure 2.1 is the basic elements of a PMU. Voltage and current are obtained from

instrument transformers which convert the magnitude of signals to the working range of the PMU. Before the analog signal is converted to digital form, it is pre-processed by the anti-aliasing filter. The anti-aliasing filter ensures that input of A/D converter has maximum frequency smaller than haft the sampling rate, which is the Nyquist frequency. Using the anti-alias filter will minimize the effect of high frequency noise in the digital signal.

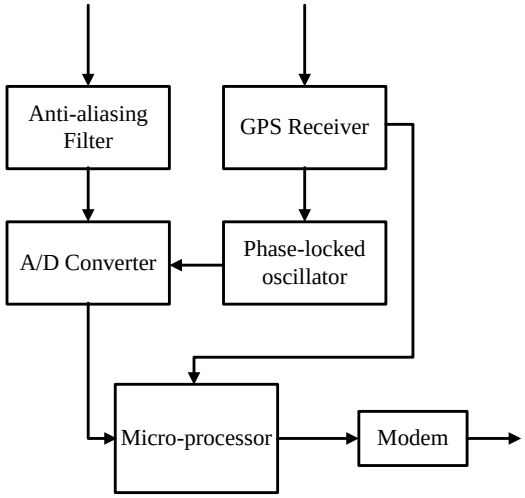


Figure 2.1: Configuration of a Phasor Measurement Unit

The sampling clock is synchronized with GPS clock pulse. GPS stands for Global Positioning System which is the system of satellites that provides precise location and time information. GPS information has been used widely in both military and civilian applications. Application utilizes location information provided by GPS can be seen daily like cell phones and cars. For the PMU, the GPS satellites provide the one pulse per second. Signal from the satellites is received by the GPS Receiver and it will convert the GPS time to the UTC clock time which takes into account the earth's rotation. Digital

numbers represent the input waveforms are stamped with the time frame synchronized with GPS clock pulses. The phasors of input signals are then computed by the micro-processor. The classical method for phasor estimation is described in the next section. The estimates are time stamped and are transmitted to higher level of monitoring system through the modem. Frequency, rate of change of frequency, flag (to indicate bad data) can also be included.

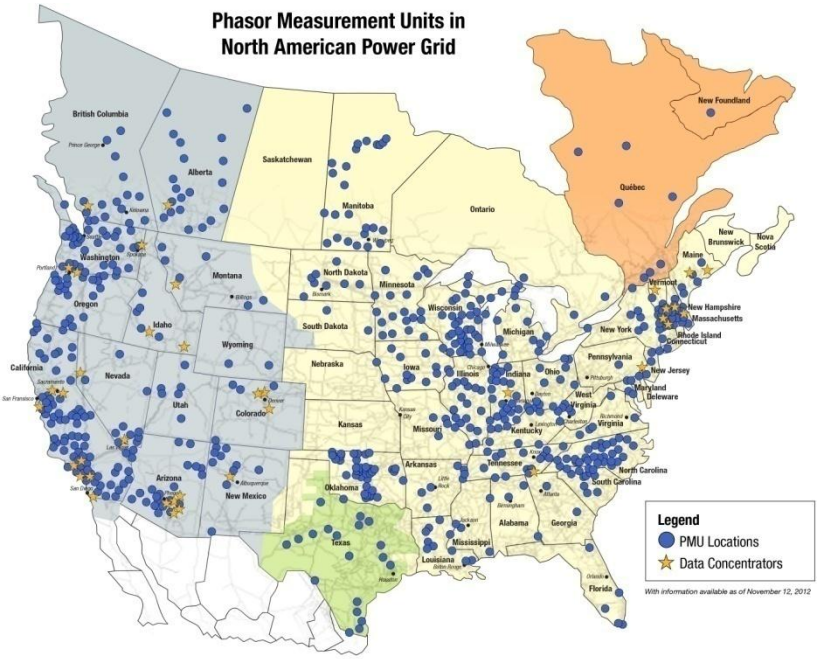


Figure 2.2: Phasor Measurement Units in North American Power Grid

The number of PMUs installed in North American power grid has been increasing. The deployment of PMUs across the network enables a better way to monitor modern power systems, called Wide Area Monitoring (WAMS). In supervisory control and data acquisition system (SCADA) which monitors traditional power system, measurements like voltage and current magnitude, active power, reactive power at different locations

and other important information are updated to the center once every two to four seconds [16]. In Wide Area Monitoring system, measurements from PMUs can be updated at a rate of once every one or two cycles, which is equal to 30 or 60 updates a second. This higher rate of report enables the monitoring system to record faster dynamic behavior in power systems.

## 2.2. PHASOR ESTIMATION USING DISCRETE FOURIER TRANSFORM

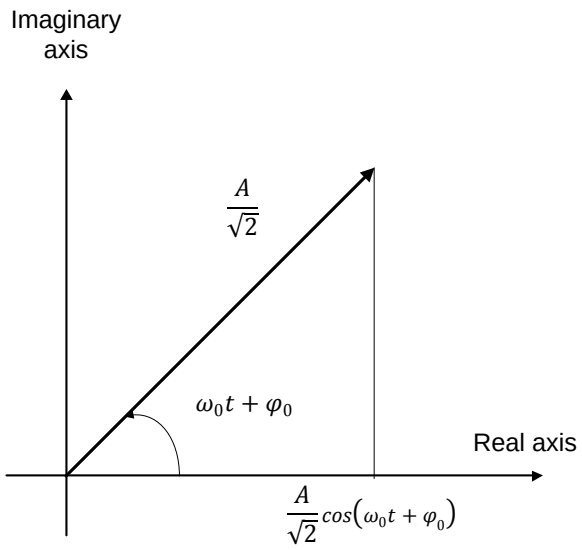


Figure 2.3: Phasor diagram

The term phasor was first introduced by C. P. Steinmetz in 1893. Phasor is the vector representing a sinusoidal function whose frequency and amplitude are time invariant. Phasors are used to represent current and voltage signals in power systems. Signal $x(t) = Acos(\omega_0 t + \varphi_0)$ can be represented by a vector in complex coordination with amplitude $\frac{A}{\sqrt{2}}$ and phase angle $\omega_0 t + \varphi_0$ (Figure 2.3). Phasor can be expressed in polar form $\frac{A}{\sqrt{2}} \angle (\omega_0 t + \varphi_0)$ or exponential form $\frac{A}{\sqrt{2}} e^{\omega_0 t + \varphi_0}$ or in rectangular

form $\frac{A}{\sqrt{2}}cos(\omega_0 t + \varphi_0) + j\frac{A}{\sqrt{2}}sin(\omega_0 t + \varphi_0)$. When the phasor is referred to not in a specific time, the time dependent part of the phase angle can be neglected. It can be simply written as $\frac{A}{\sqrt{2}}\angle\varphi_0$ in polar form. Now the phasor becomes a time invariant vector, assuming the system is in steady state. This makes the calculation much easier compared to the using of instantaneous voltage and current signals. In this thesis, however, the phasor is referred to as a time varying quantity because it is intended to be used in power system monitoring.

### 2.2.1. PHASOR ESTIMATION OF NOMINAL FREQUENCY SIGNAL

Consider the input of the estimator is an ideal sinusoidal signal at nominal frequency $f_0$. Angular frequency is $\omega_0 = 2\pi f_0$.

$$x(t) = Acos(\omega_0 t + \varphi_0) \tag{2.1}$$

The signal is sampled at a sampling frequency which is a multiple of nominal frequency $f_s = Nf_0$. For current and voltage waveforms of electric grid, the nominal frequency is 50Hz in most part of the world and is 60 Hz in the United States. This allows PMU designers to select sampling frequency for each system. The sampled data of input signal is:

$$\begin{aligned} x(n) &= Acos(\omega_0 nT_s + \varphi_0) \\ &= Acos\left(\frac{2\pi n}{N} + \varphi_0\right) \end{aligned} \tag{2.2}$$

Consider the first cycle of input signal, which is the first N samples from $n = 0$ to $n = N - 1$. The fundamental component of this data window is computed using Discrete Fourier Transform.

$$X_0 = \frac{1}{N}\sum_{n=0}^{N-1} x(n)e^{-j\frac{2\pi}{N}n}$$

$$= \frac{A}{N}\sum_{n=0}^{N-1}\left(cos\left(\frac{2\pi n}{N}+\varphi_0\right)cos\left(\frac{2\pi n}{N}\right) - jcos\left(\frac{2\pi n}{N}+\varphi_0\right)sin\left(\frac{2\pi n}{N}\right)\right)$$

$$= \frac{A}{2N}\sum_{n=0}^{N-1}\left(cos\left(\frac{4\pi n}{N}+\varphi_0\right) + cos(\varphi_0) - jsin\left(\frac{2\pi n}{N}+\varphi_0\right) + jsin(\varphi_0)\right) \quad (2.3)$$

Because the summation $\sum_{n=0}^{N-1} cos\left(\frac{4\pi n}{N}+\varphi_0\right)$ and $\sum_{n=0}^{N-1} sin\left(\frac{4\pi n}{N}+\varphi_0\right)$ are equal to zero, (2.3) becomes:

$$X_0 = \frac{A}{2}e^{j\varphi_0} \quad (2.4)$$

As the phasor representation is defined in 2.1, we need to adjust equation (2.3) to calculate the phasor representation of data window $n = 0,1,2,\dots,N-1$ or $t \in [0,1/f_0]$.

$$X_0 = \frac{\sqrt{2}}{N}\sum_{n=0}^{N-1} x(n)e^{-j\frac{2\pi}{N}n} \quad (2.5)$$

The phasor representation of the sampled signal $x(n)$ can be calculated using the above formula simply by moving the data window on time domain. This is called non-recursive update method. For this method, phasor representation of each data window is calculated independently. As a result, error of estimation does not accumulate.

$$X_r = \frac{\sqrt{2}}{N}\sum_{n=r}^{r+N-1} x(n)e^{-j\frac{2\pi}{N}(n-r)} \quad (2.6)$$

Another method is recursive updates. For this method, phasor representation of a data window is updated using the phasor obtained from previous step. Recursive update

formula can be derived from (2.6):

$$X_{r+1} = \frac{\sqrt{2}}{N}\sum_{n=r+1}^{r+N} x(n)e^{-j\frac{2\pi}{N}(n-r-1)}$$

$$= \left(\frac{\sqrt{2}}{N}\sum_{n=r}^{r+N-1} x(n)e^{-j\frac{2\pi}{N}(n-r)}\right)e^{-j\frac{2\pi}{N}} + \frac{\sqrt{2}}{N}e^{-j\frac{2\pi}{N}}\big(x(r+N) - x(r)\big)$$

$$= \left(X_{r+1} + \frac{\sqrt{2}}{N}x(r+N) - \frac{\sqrt{2}}{N}x(r)\right)e^{-j\frac{2\pi}{N}} \tag{2.7}$$

Using recursive update method can reduce the computation burden as there is no need to calculate the loop $n = r, r+1, r+2, \dots, r+N-1$. However, because the error is added in each update, the phasor estimation obtained by this method is not reliable. This accumulated error can be reduced by calculating a new phasor representation using non-recursive method after repeat the recursive updates a certain times.

### 2.2.2. PHASOR ESTIMATION OF OFF-NOMINAL FREQUENCY SIGNAL

Now, consider the input of the phasor estimator is an ideal sinusoidal signal with frequency $f_x \neq f_0$. Angular frequency is $\omega_0 = 2\pi f_0$.

$$x(t) = Acos(\omega_x t + \varphi_0) \tag{2.8}$$

The signal $x(t)$ is sampled with frequency $f_s = Nf_0$. This means $T_s = T_0/N$

$$x(n) = Acos(\omega_x n T_s + \varphi_0) \tag{2.9}$$

Using non-recursive method described in 2.2.1, the estimated phasor representation of the data window is expressed as:

$$X_r' = \frac{A}{\sqrt{2}N}\sum_{n=r}^{r+N-1}\left(e^{j(\omega_x nT_s+\varphi_0)} + e^{-j(\omega_x nT_s+\varphi_0)}\right)e^{-j\frac{2\pi}{N}(n-r)}$$

$$= \frac{A}{\sqrt{2}}e^{j(\omega_x nT_s+\varphi_0)}\frac{1}{N}\sum_{n=0}^{N-1}e^{j\left(\omega_x nT_s-\frac{2\pi}{N}n\right)}$$

$$+\frac{A}{\sqrt{2}}e^{-j(\omega_x nT_s+\varphi_0)}\frac{1}{N}\sum_{n=0}^{N-1}e^{-j\left(\omega_x nT_s+\frac{2\pi}{N}n\right)}$$

$$= X_r P + X_r^* Q \tag{2.10}$$

with

$$P = \frac{1}{N}\sum_{n=0}^{N-1}e^{j\left(\omega_x nT_s-\frac{2\pi}{N}n\right)} = \frac{1}{N}\sum_{n=0}^{N-1}e^{j(\omega_x-\omega_0)nT_s} = \frac{e^{jN(\omega_x-\omega_0)T_s}-1}{N(e^{j(\omega_x-\omega_0)T_s}-1)}$$

$$Q = \frac{1}{N}\sum_{n=0}^{N-1}e^{-j\left(\omega_x nT_s+\frac{2\pi}{N}n\right)} = \frac{1}{N}\sum_{n=0}^{N-1}e^{j(\omega_x+\omega_0)nT_s} = \frac{e^{jN(\omega_x+\omega_0)T_s}-1}{N(e^{j(\omega_x+\omega_0)T_s}-1)}$$

Assuming the frequency $\omega_x$ is estimated accurately, $P$ and $Q$ can be computed. In (2.10), $X_r'$ is known ($X_r'$ is calculated using non-recursive update method (2.5)). What we need to do is to find phasor $X_r$. (2.10) is re-written as:

$$\begin{cases} X_r' = X_r P + X_r^* Q \\ X_r'^* = X_r Q^* + X_r^* P^* \end{cases} \tag{2.11}$$

From (2.11), phasor $X_0$ is obtained as:

$$X_r = \frac{P^* X_r' - Q X_r'^*}{PP^* - QP^*} \tag{2.12}$$

## 2.3. FREQUENCY ESTIMATION

In the electric grid, frequency is regulated to ensure it remains nearly constant. Speed

governor at each generator will response to changes in the network to balance the input mechanical power and the generated power. As a result, events like fault on transmission lines, load changes, generator loss, etc. can be characterized by looking at the frequency waveforms.

Historically, frequency in power systems is measured using mechanical speed sensor. Devices are installed at power plants to measure speed of rotation of generators. This limits the frequency measurement at the generator site. In modern power systems, frequency can be measured at any point throughout the network. Instantaneous voltage waveforms are recorded at high sampling rate and there are many different methods to estimate the frequency digitally. Frequency estimation method using phasor angle is described in this section.

Using non-recursive update method, the phasor is estimated from a data window which has length equal to one cycle of nominal frequency using (2.6). The estimated phasor obtained from (2.6) $X_r'$ depends on the input signal's frequency $\omega_x$ and the sampling rate $f_s$, which is related to the nominal frequency $f_0$.

$$X_r' = \frac{A}{\sqrt{2}} e^{j(\omega_x r T_s + \varphi_0)} \frac{e^{jN(\omega_x - \omega_0)T_s} - 1}{N(e^{j(\omega_x - \omega_0)T_s} - 1)} + \frac{A}{\sqrt{2}} e^{-j(\omega_x r T_s + \varphi_0)} \frac{e^{jN(\omega_x + \omega_0)T_s} - 1}{N(e^{j(\omega_x + \omega_0)T_s} - 1)} \tag{2.13}$$

$X_r'$ is summation of two addends, one is proportional to $e^{j(\omega_x n T_s + \varphi_0)}$ and the other is proportional to $e^{-j(\omega_x n T_s + \varphi_0)}$. Notice that:

$$\lim_{\omega_x \to \omega_0} \frac{e^{jN(\omega_x-\omega_0)T_s}-1}{N(e^{j(\omega_x-\omega_0)T_s}-1)} = 1 \tag{2.14}$$

$$\lim_{\omega_x \to \omega_0} \frac{e^{jN(\omega_x+\omega_0)T_s}-1}{N(e^{j(\omega_x+\omega_0)T_s}-1)} = 0 \tag{2.15}$$

(3.1) and (3.2) shows that when the frequency of input signal approaches nominal frequency, $X_r'$ approaches the accurate value of phasor representation $\frac{A}{\sqrt{2}}e^{j(\omega_x nT_s+\varphi_0)}$. Define $\phi_r$ is the angle of complex number $X_r'$, we have the approximation:

$$\phi_r \approx \omega_x r T_s + \varphi_0 \tag{2.16}$$

For the set of samples with $n = r+1, r+2, \dots, r+N$, the angle of $X_{r+1}'$ is:

$$\phi_{r+1} \approx \omega_x (r+1) T_s + \varphi_0 \tag{2.17}$$

From (2.16) and (2.17), the system frequency can be computed with $\omega_x = \frac{\phi_{r+1}-\phi_r}{T_s}$, or:

$$f = \frac{1}{2\pi}\frac{d\phi}{dt} \tag{2.18}$$

In commercial phasor measurement units (e.g. from ABB, SEL), rate of change of frequency is estimated also:

$$\frac{df}{dt} = \frac{1}{2\pi}\frac{d^2\phi}{dt^3} \tag{2.19}$$

One issue with this method is the existing of ripple caused by the component proportional to $e^{-j(\omega_x nT_s+\varphi_0)}$ in $X_r'$. To reduce the error, a digital filter may need to be applied. The simplest filter can be used is an average filter. In [9], IEEE standard C37.118.1-2011 defines two performance classes: P class and M class. Phasor measurement units in M class are used for application requiring greater precision but no

minimal report delay. P class on the other hand required fast response therefore mandates no explicit filter. Comparison of maximum error of frequency estimated by different methods will be discussed in the next chapter.

# CHAPTER 3

## NOVEL METHOD FOR PRECISE FREQUENCY MEASUREMENT

As discussed in 2.2.2, the estimated phasor can be compensated assuming frequency is known or is estimated accurately. Now, the accuracy of phasor measurement units depends on how precise the frequency estimation is. In this section, the classical method, using phase angle analysis, has been presented. Beside this method, many other algorithms have been proposed to measure frequency in power system, includes least square estimation, leakage coefficient measurement [10], Kalman filtering [13], Neural Network [12] , Wavelet analysis [14], etc.

Most of the frequency measurement techniques use Discrete Fourier Transform at fundamental frequency (nominal frequency of power system) and then using different method to remove error caused by off nominal frequency and noise. Because the first step is to calculate DFT component at nominal frequency, the accuracy of the above methods decreases significantly when signal is highly off-nominal and especially under transient condition.

In [10], instead of using DFT term at fundamental frequency only, the authors used the leakage coefficient to calculate the variation of signal from nominal frequency:

$$\eta = \frac{\sum_{k=0}^{N-1}(|X(k)| - |X(1)|)}{|X(1)|} \tag{3.1}$$

$$\Delta f = \frac{\eta}{0.095584345} \tag{3.2}$$

Since the relation in (3.2) is correct only if the signal is sinusoidal and the data window starts from phase $\frac{\pi}{2}$. As a result, a zero crossing detector must be applied. This makes the method sensitive to noise.

In this chapter, the frequency components of an input signal at off nominal frequency will be analyzed. Our analysis shows that by using several DFT terms in a linear combination, the phase angle of input signal is estimated with smaller error. This also means frequency estimate is more accurate.

## 3.1. Fourier Series of a Periodic Continuous Time Signal at Off Nominal Frequency

To measure the frequency which may be time variant, we will truncate the signal by a rectangular window with length equal to nominal period and then, slide the window over time. Without loss of generality, the signal was considered in one nominal period $[0, T_0]$. Assume that in this time interval, the signal is an ideal sinusoidal function.

$$x(t) = A\cos(\omega_x t + \varphi_0) \tag{3.3}$$

The rectangular window:

$$\mathrm{rect}_{[0,T_0]}(t) = \begin{cases} 1 & t \in [0, T_0] \\ 1 & t \notin [0, T_0] \end{cases} \tag{3.4}$$

Fourier transform of windowing function:

$$\mathrm{FT}\{\mathrm{rect}_{[0,T_0]}(t)\} = \frac{\sin\left(\omega \frac{T_0}{2}\right)}{\frac{\omega}{2}} e^{-j\omega\frac{T_0}{2}} \tag{3.5}$$

According to modulation theorem, Fourier transform of truncated signal is:

$$FT\{x(t).rect_{[0,T_0]}(t)\} = \frac{A}{2}e^{j\varphi_0}\frac{\sin\left((\omega-\omega_x)\frac{T_0}{2}\right)}{\frac{(\omega-\omega_x)}{2}}e^{-j(\omega-\omega_x)\frac{T_0}{2}} + \frac{A}{2}e^{-j\varphi_0}\frac{\sin\left((\omega+\omega_x)\frac{T_0}{2}\right)}{\frac{(\omega+\omega_x)}{2}}e^{-j(\omega+\omega_x)\frac{T_0}{2}} \quad (3.6)$$

Consider $\tilde{x}(t)$ is a periodic signal:

$$\tilde{x}(t+nT_0) = x(t).rect_{[0,T_0]}(t) \quad t\in[0,T_0], t\in Z \quad (3.7)$$

Fourier series of $\tilde{x}(t)$:

$$FS\{\tilde{x}(k)\} = \frac{1}{T_0}FT\{x(t).rect_{[0,T_0]}(t)\}_{|\omega=k\frac{2\pi}{T_0}}$$

$$= \frac{A}{2}sin\left(\pi\frac{\Delta\omega}{\omega_0}\right)e^{j\left(\varphi_0+\pi\frac{\Delta\omega}{\omega_0}\right)}\frac{1}{\pi\left(\frac{\Delta\omega}{\omega_0}+1-k\right)}$$

$$+\frac{A}{2}sin\left(\pi\frac{\Delta\omega}{\omega_0}\right)e^{-j\left(\varphi_0+\pi\frac{\Delta\omega}{\omega_0}\right)}\frac{1}{\pi\left(\frac{\Delta\omega}{\omega_0}+1+k\right)} \quad (3.8)$$

Note that the function $\tilde{x}(t)$ is obtained by repeating the truncated part of $x(t)$ in time interval $[0,T_0]$. Because the period of $x(t)$ is $T_x \neq T_0$, the function $\tilde{x}(t)$ is not sinusoidal. The Fourier series of a continuous signal cannot be computed in digital micro-processor. However, as it will be shown in the following section, Fourier series expressed in (3.8) is closely related to the discrete Fourier transform which can be computed from a set of discrete samples.

Another remark about (3.8) is the summation of two terms; the first term

$\frac{A}{2}sin\left(\pi\frac{\Delta\omega}{\omega_0}\right)e^{j\left(\varphi_0+\pi\frac{\Delta\omega}{\omega_0}\right)}\frac{1}{\pi\left(\frac{\Delta\omega}{\omega_0}+1-k\right)}$ has phase angle $\varphi_0+\pi\frac{\Delta\omega}{\omega_0}$ and the second term $\frac{A}{2}sin\left(\pi\frac{\Delta\omega}{\omega_0}\right)e^{-j\left(\varphi_0+\pi\frac{\Delta\omega}{\omega_0}\right)}\frac{1}{\pi\left(\frac{\Delta\omega}{\omega_0}+1+k\right)}$ has phase angle $-j\left(\varphi_0+\pi\frac{\Delta\omega}{\omega_0}\right)$. When $k=1$, the magnitude of second term becomes $\frac{A}{2}sin\left(\pi\frac{\Delta\omega}{\omega_0}\right)\frac{1}{\pi\left(\frac{\Delta\omega}{\omega_0}+1\right)}$ which is nearly zero since $sin\left(\pi\frac{\Delta\omega}{\omega_0}\right)\approx 0$ when $\frac{\Delta\omega}{\omega_0}$ is small. If the second term is equal to zero, the frequency can be calculated simply from the phase angle of $FS\{\tilde{x}(1)\}$. However, depending on the frequency of input signal, the second term still changes the phase angle of the summation from $\varphi_0+\pi\frac{\Delta\omega}{\omega_0}$. A method to eliminate the second term is discussed in the following section.

## 3.2. Discrete Fourier Transform at Off Nominal Frequency

The signal $x(t)$ in equation (3.3) is sampled with sampling frequency $f_s=Nf_0$ where $f_0$ is nominal frequency.

$$x(n)\ =Acos(\omega_x nT_s+\varphi_0) \tag{3.9}$$

In discrete time domain, the periodic signal $\tilde{x}(t)$ mentioned in (3.7) becomes

$$\tilde{x}(n+kN)=x(n)\quad n\in[0,N-1],k\in Z \tag{3.10}$$

Discrete Fourier Transform of $\tilde{x}(n)$:

$$\tilde{X}(k)=\frac{1}{N}\sum_{n=0}^{N-1}x(n)e^{-j\frac{2\pi}{N}nk} \tag{3.11}$$

When $k=1$, (3.11) becomes the formula to calculate the phasor mentioned in previous chapter. The input signal can be expressed as $x(n)=\frac{A}{2}e^{j(\omega_x nT_s+\varphi_0)}+\frac{A}{2}e^{-j(\omega_x nT_s+\varphi_0)}$.

Substitute to (3.11):

$$\tilde{X}(k) = \frac{1}{N}\sum_{n=0}^{N-1}\left(\frac{A}{2}e^{j(\omega_x nT_s+\varphi_0)} + \frac{A}{2}e^{-j(\omega_x nT_s+\varphi_0)}\right)e^{-j\frac{2\pi}{N}nk} \tag{3.12}$$

Substitute $\frac{2\pi}{N} = \omega_0$ and $\Delta\omega = \omega_x - \omega_0$, after several steps of derivation we get:

$$\tilde{X}(k) = \frac{A}{2N}sin\left(\pi\frac{\Delta\omega}{\omega_0}\right)(-1)^{k+1}e^{-jk\frac{N-1}{N}\pi}\left(\frac{e^{j\left(\varphi_0+\left(\frac{\Delta\omega}{\omega_0}+1\right)\frac{N-1}{N}\pi\right)}}{sin\left(\left(\frac{\Delta\omega}{\omega_0}+1-k\right)\frac{\pi}{N}\right)}\right.$$

$$\left. + \frac{e^{-j\left(\varphi_0+\left(\frac{\Delta\omega}{\omega_0}+1\right)\frac{N-1}{N}\pi\right)}}{sin\left(\left(\frac{\Delta\omega}{\omega_0}+1+k\right)\frac{\pi}{N}\right)}\right) \tag{3.13}$$

(3.13) will become Fourier series of $\tilde{x}(n)$ when the number of samples per cycle goes to infinity $N \to \infty$. (3.13) is modified to obtained the form which is similar to the Fourier series (3.8).

$$\tilde{Y}(k) = \tilde{X}(k)(-1)^{k+1}e^{jk\frac{N-1}{N}\pi}$$

$$= \frac{A}{2N}sin\left(\pi\frac{\Delta\omega}{\omega_0}\right)\left(\frac{e^{j\left(\varphi_0+\left(\frac{\Delta\omega}{\omega_0}+1\right)\frac{N-1}{N}\pi\right)}}{sin\left(\left(\frac{\Delta\omega}{\omega_0}+1-k\right)\frac{\pi}{N}\right)} + \frac{e^{-j\left(\varphi_0+\left(\frac{\Delta\omega}{\omega_0}+1\right)\frac{N-1}{N}\pi\right)}}{sin\left(\left(\frac{\Delta\omega}{\omega_0}+1+k\right)\frac{\pi}{N}\right)}\right) \tag{3.14}$$

## 3.3. Linear Combination of Discrete Fourier Transform Terms

From the equation (3.13) or (3.14), it can be seen that $\tilde{X}(k)$ and $\tilde{Y}(k)$ are linear combinations of two complex conjugates. This section will discuss how the combination of Discrete Fourier Transform at different frequencies can reduce the negative angle

components; hence reduce the frequency estimation errors. The algorithm is basically based on the following problem:

$$S = \frac{c_0}{r+m_0} + \frac{c_1}{r+m_1} + \cdots + \frac{c_l}{r+m_{l-1}} \quad c_1 = 1, m_i \neq 0 \tag{3.15}$$

Find coefficient $c_i$ so that $S$ can be expressed as:

$$S = \frac{a_{l-1}r^{l-1}}{(r+m_0)(r+m_1)\ldots(r+m_{l-1})} \tag{3.16}$$

Generally, the numerator of S is a polynomial $a_{l-1}r^{l-1} + a_{l-2}r^{l-2} + \cdots + a_1 r + a_0$. We need to find $\{c_i\}$ so that $a_{l-2} = a_{l-3} = \cdots = a_0 = 0$ and $a_{l-1} \neq 0$.

The solution for this problem is:

$$\begin{bmatrix} c_0 \\ c_2 \\ c_3 \\ \cdots \\ c_{l-1} \end{bmatrix} = \begin{bmatrix} \frac{1}{m_0} & \frac{1}{m_2} & \frac{1}{m_3} & \cdots & \frac{1}{m_{l-1}} \\ \left(\frac{1}{m_0}\right)^2 & \left(\frac{1}{m_2}\right)^2 & \left(\frac{1}{m_3}\right)^2 & \cdots & \left(\frac{1}{m_{l-1}}\right)^2 \\ \left(\frac{1}{m_0}\right)^3 & \left(\frac{1}{m_2}\right)^3 & \left(\frac{1}{m_3}\right)^3 & \cdots & \left(\frac{1}{m_{l-1}}\right)^3 \\ \cdots & \cdots & \cdots & \cdots & \cdots \\ \left(\frac{1}{m_0}\right)^{l-1} & \left(\frac{1}{m_2}\right)^{l-1} & \left(\frac{1}{m_3}\right)^{l-1} & \cdots & \left(\frac{1}{m_{l-1}}\right)^{l-1} \end{bmatrix} \times \begin{bmatrix} -\frac{1}{m_1} \\ -\left(\frac{1}{m_1}\right)^2 \\ -\left(\frac{1}{m_1}\right)^3 \\ \cdots \\ -\left(\frac{1}{m_1}\right)^{l-1} \end{bmatrix} \tag{3.17}$$

Note that when $r$ is small, the value of $S$ is proportional to $r^{l-1}$ which is much very small and can be considered zero. This characteristic will be used to eliminate the term with phase angle $-\left(\varphi_0 + \left(\frac{\Delta\omega}{\omega_0} + 1\right)\frac{N-1}{N}\pi\right)$ in (3.14).

Suppose we select the set $\{k_0, k_1, k_2, \ldots, k_{l-1}\}$. Then we have the set of modified discrete Fourier transform components $\{\tilde{Y}(k_0), \tilde{Y}(k_1), \tilde{Y}(k_2), \ldots, \tilde{Y}(k_{l-1})\}$. From the definition of discrete Fourier transform, $k_i$ must be integer. A linear combination of $\{\tilde{Y}(k_i)\}$ is defined:

$$\mathrm{C} = \mathrm{c}_0\widetilde{\mathrm{Y}}(\mathrm{k}_0) + \mathrm{c}_1\widetilde{\mathrm{Y}}(\mathrm{k}_1) + \cdots + \mathrm{c}_{\mathrm{l}-1}\widetilde{\mathrm{Y}}(\mathrm{k}_{\mathrm{l}-1}) \quad \text{with } \mathrm{c}_1 = 1 \tag{3.18}$$

Substitute (3.14) to (3.18):

$$C = \frac{A}{2N} sin\left(\pi \frac{\Delta\omega}{\omega_0}\right)\left(Ue^{j\psi} + Ve^{-j\psi}\right) \tag{3.19}$$

with

$$\psi = \varphi_0 + \left(\frac{\Delta\omega}{\omega_0} + 1\right)\frac{N-1}{N}\pi \tag{3.20}$$

$$U = \frac{c_0}{sin\left(\left(\frac{\Delta\omega}{\omega_0} + 1 - k_0\right)\frac{\pi}{N}\right)} + \frac{c_1}{sin\left(\left(\frac{\Delta\omega}{\omega_0} + 1 - k_1\right)\frac{\pi}{N}\right)} + \cdots + \frac{c_l}{sin\left(\left(\frac{\Delta\omega}{\omega_0} + 1 - k_{l-1}\right)\frac{\pi}{N}\right)} \tag{3.21}$$

$$V = \frac{c_0}{sin\left(\left(\frac{\Delta\omega}{\omega_0} + 1 + k_0\right)\frac{\pi}{N}\right)} + \frac{c_1}{sin\left(\left(\frac{\Delta\omega}{\omega_0} + 1 + k_1\right)\frac{\pi}{N}\right)} + \cdots + \frac{c_l}{sin\left(\left(\frac{\Delta\omega}{\omega_0} + 1 + k_{l-1}\right)\frac{\pi}{N}\right)} \tag{3.22}$$

To reduce the negative angle component in (3.20), $V$ should be minimized. Using the result from (3.17) with $r = sin\left(\frac{\pi\Delta\omega}{N\omega_0}\right)$, the coefficients $\{c_i\}$ is found as shown in (3.23).

$$\begin{bmatrix} c_0 \\ c_2 \\ c_3 \\ \dots \\ c_{l-1} \end{bmatrix} = \frac{1}{cos\left((1+k_1)\frac{\pi}{N}\right)} \begin{bmatrix} cos\left((1+k_0)\frac{\pi}{N}\right) \\ cos\left((1+k_2)\frac{\pi}{N}\right) \\ cos\left((1+k_3)\frac{\pi}{N}\right) \\ \dots \\ cos\left((1+k_{l-1})\frac{\pi}{N}\right) \end{bmatrix}$$

$$(\times) \begin{bmatrix} cot\left((1+k_0)\frac{\pi}{N}\right) & cot\left((1+k_2)\frac{\pi}{N}\right) & \dots & cot\left((1+k_{l-1})\frac{\pi}{N}\right) \\ cot^2\left((1+k_0)\frac{\pi}{N}\right) & cot^2\left((1+k_2)\frac{\pi}{N}\right) & \dots & cot^2\left((1+k_{l-1})\frac{\pi}{N}\right) \\ cot^3\left((1+k_0)\frac{\pi}{N}\right) & cot^3\left((1+k_2)\frac{\pi}{N}\right) & \dots & cot^3\left((1+k_{l-1})\frac{\pi}{N}\right) \\ \dots & \dots & \dots & \dots \\ cot^{l-1}\left((1+k_0)\frac{\pi}{N}\right) & cot^{l-1}\left((1+k_2)\frac{\pi}{N}\right) & \dots & cot^{l-1}\left((1+k_{l-1})\frac{\pi}{N}\right) \end{bmatrix}$$

$$\times \begin{bmatrix} -cot\left((1+k_1)\frac{\pi}{N}\right) \\ -cot^2\left((1+k_1)\frac{\pi}{N}\right) \\ -cot^3\left((1+k_1)\frac{\pi}{N}\right) \\ \dots \\ -cot^{l-1}\left((1+k_1)\frac{\pi}{N}\right) \end{bmatrix} \tag{3.23}$$

Now, the frequency is calculated from phase angle of vector $C$. Call $\theta$ is phase angle of $C$, the frequency estimate is:

$$f = \frac{1}{2\pi}\frac{d\theta}{dt} \tag{3.24}$$

## 3.4. SELECTION OF DISCRETE FOURIER TRANSFORM TERMS

This section will discuss the selection of discrete flourier transform terms (selection

of $\{k_i\}$) to archive accurate estimation. As described in section 3.3, with a set of DFT terms selected, coefficient $c_i$ for each term can be found using (3.23) so that the component $Ve^{-j\psi}$ in (3.19) is small and can be neglected. If $Ve^{-j\psi}$ is equal to zero then there is no error caused by the off-nominal frequency. However, in reality, the accuracy of frequency estimate depends on how small $Ve^{-j\psi}$ is in comparison with $Ue^{j\psi}$. Hence, the selection of set $\{k_i\}$ has to consider the value of $\left|\frac{U}{V}\right|$.

From practical point of view, the error of frequency estimate does not only come from the off-nominal frequency of input signal but also from measurement noise or harmonic components of voltage and current waveform. When there is noise, each DFT term calculated by (3.14) will have an error added. Assuming the error added for each DFT term is equal, the total error added to $C$ in (3.19) is proportional to sum of absolute value of coefficients $\sum_i |c_i|$. Because we only need to calculate the phase angle of component $Ue^{j\psi}$, the error of the estimation is proportional to $\sum_i \left|\frac{c_i}{U}\right|$.

The "normalized" values of $\left|\frac{U}{V}\right|$ and $\sum_i \left|\frac{c_i}{U}\right|$ for some sets of $\{k_i\}$ is shown in Table 3.1. "Normalized" here means values of $\left|\frac{U}{V}\right|$ and $\sum_i \left|\frac{c_i}{U}\right|$ are divided to the corresponding value when only the DFT term at fundamental frequency are used . Depending on each particular application that the device is intended to be used, the designer may select the appropriate set $\{k_i\}$.Some applications may have better instrument transformer so the noise is not a big problem. Other application may have higher noise level so the error caused by noise in input signal is a concern. In addition, the burden of computation needs to be considered as well. Including more DFT terms in the estimation also means higher performance computing device is needed.

Table 3.1:Selection of DFT terms

$$C = c_0\tilde{Y}(k_0) + c_1\tilde{Y}(k_1) + \cdots + c_{l-1}\tilde{Y}(k_{l-1})$$
$$= \frac{A}{2N}\sin\left(\pi\frac{\Delta\omega}{\omega_0}\right)\left(Ue^{j\psi} + Ve^{-j\psi}\right)$$

| No | $\{k_i\}$ | $\{c_i\}$ | $U_n$ | $V_n$ | $\left\|\frac{U_n}{V_n}\right\|$ | $\sum_i \left\|\frac{c_i}{U_n}\right\|$ |
|---|---|---|---|---|---|---|
| 1 | 1 | 0, 1 | 1 | 1 | 1 | 1 |
| 2 | 0, 1 | -0.5002, 1 | 0.9917 | 0.0081 | 120.9246 | 1.5126 |
| 3 | 0, 2 | -0.3337, 1 | 0.0224 | 0.0073 | 3.0638 | 59.474 |
| 4 | 1, 2 | -0.6672, 1 | 0.6841 | 0.0018 | 3.70E+02 | 2.4369 |
| 5 | 1, 3 | -0.5009, 1 | 0.5093 | 0.002 | 2.44E+02 | 2.9466 |
| 6 | -2, 1 | 0.5002 1 | 1.0027 | -0.0254 | 39.4683 | 1.4961 |
| 7 | 0, 1, 2 | -0.1251, 1, -1.1237 | 1.017 | 2.27E-05 | .48E+04 | 42.2113 |
| 8 | 0, 1, 3 | -0.1669, 1, -1.3298 | 1.0084 | 3.41E-05 | 2.96E+04 | 2.4759 |
| 9 | -2, 0, 1 | -0.3337, 1, -2.6662 | 2.6516 | 5.56E-04 | 4.77E+03 | 1.5085 |
| 10 | -2, 1, 2 | -0.0627, 1, -1.6867 | 1.0282 | 7.03E-05 | 1.46E+04 | 2.6739 |
| 11 | -2 1 3 | -0.1004 1 -2.3968 | 1.0196 | 1.06E-04 | 9.65E+03 | 3.4301 |
| 12 | 1 2 3 | -0.2227 1 -0.8873 | 0.2322 | 2.56E-06 | 9.05E+04 | 9.0873 |
| 13 | 0, 1, 2, 3 | -0.042, 1, -3.37, 2.65 | 1.034 | 9.45E-08 | 1.09E+07 | 6.8183 |
| 14 | -2, 0, 1, 2 | 0.168, 1, -10.654, 13.473 | 10.8655 | 6.15E-06 | 1.77E+06 | 2.328 |
| 15 | -2, 0, 1, 3 | 0.2, 1, -7.988, 12.756 | 8.0779 | 6.93E-06 | 1.17E+06 | 2.7166 |
| 16 | -2, 1, 2, 3 | 0.013, 1, -5.053, 4.784 | 1.0455 | 2.93E-07 | 3.57E+06 | 10.3779 |

In Table 3.1, for $\{k_i\} = \{0, 1, 3\}$, $\left|\frac{U_n}{V_n}\right| = 2.96E4$ which is very large while $\sum_i |\frac{c_i}{U_n}| = 2.4759$ which is relatively small compare to other choices. The frequency estimation result with selected DFT terms $\{k_i\} = \{0, 1, 3\}$ is shown in Figure 3.1, Figure 3.2 and Figure 3.3.

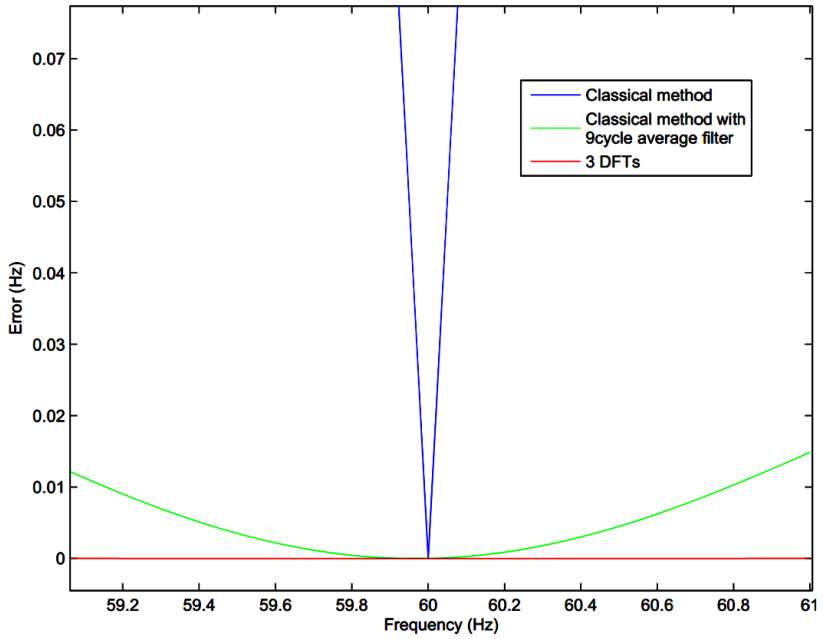


Figure 3.1: Maximum error of different frequency estimation methods

Figure 3.1 is the maximum error of frequency estimated by classical method with a 9 cycle average filter, classical method without filter and the proposed method using three DFT terms. The result is our proposed method can estimate the frequency very accurately even though no additional filter is applied. For the frequency range from 59Hz to 61 Hz, the maximum error is almost zero. For the classical method, an average filter can reduce the error significantly as discussed in chapter 2.

In Figure 3.2, the maximum error of frequency estimated by the proposed method using three DFT terms is shown in a wider range of frequency. The error is still small, less than

0.2 Hz in this range.

Figure 3.3 is the frequency estimate when input signal's frequency is varying. This can happen when the power system is transient. Figure shows that the proposed method is able to estimate the time varying frequency precisely. The error for classical method is much higher when no filter is used. When an average filter is used to reduce the error, it still cannot track the frequency accurately because the filter distorts the shape of its input waveform.

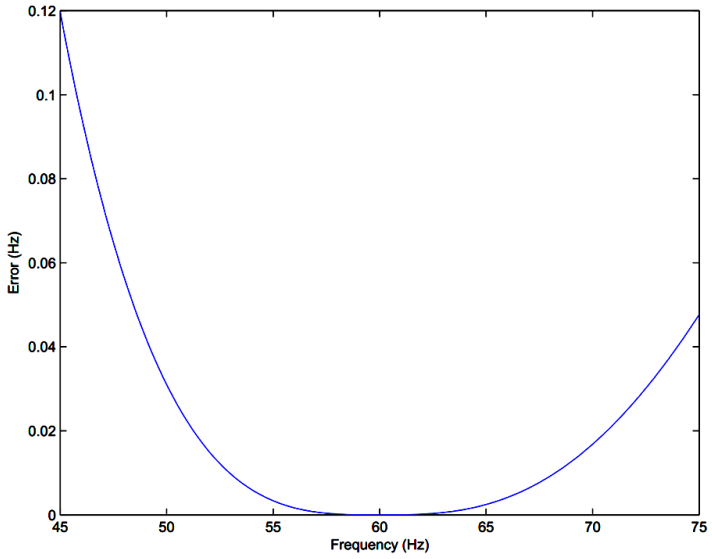


Figure 3.2: Maximum error of different frequency estimation methods

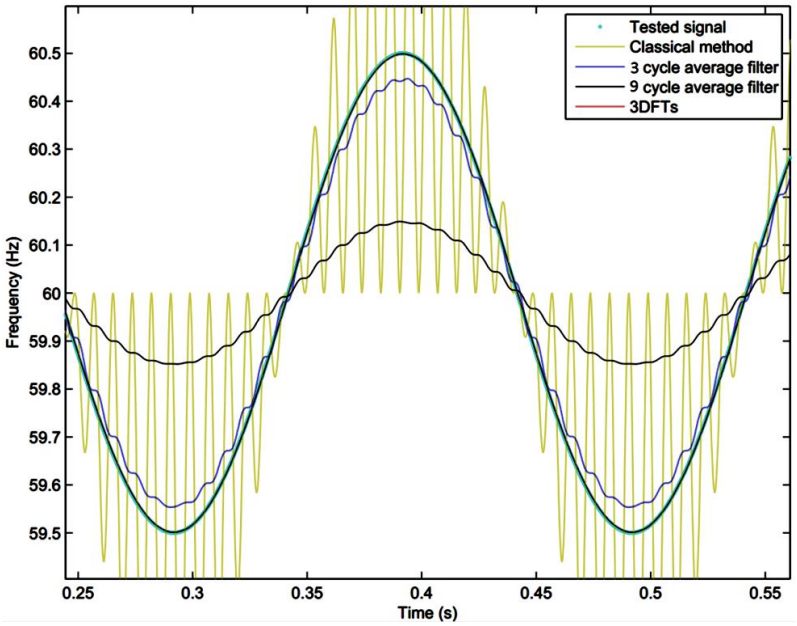


Figure 3.3: Frequency estimations of transient signal

# CHAPTER 4

# FAULT LOCATION IN POWER SYSTEM USING NETWORK IMPEDANCE MATRIX CALCULATION

## 4.1. OVERVIEW OF FAULT LOCATION IN POWER SYSTEM

The problem of fault location is closely related to power system protection. The function of protection devices is to isolate the faulted parts from the rest of the system while the function of fault locator is to find the location of fault accurately. The aim of both fault location and protection devices is to reduce or prevent damage caused by a fault, increase the quality of service and reduce overall cost of energy delivery. Fault locator and protection device both process measurements from instrumental transformers. Because of these similarities, some commercial protective relays in the market have fault location function.

When the fault occurs, there will be transient in voltage and current on the faulted line. Depending on the setting of protective relays, circuit breakers may disconnect the faulted section. Analyzing an event of fault always need to consider the operation of protection devices. In [18], the author uses breaker-clearing transient to determine fault location. For the fault location method that we will discuss in following sections of this chapter, information from protection devices such as status of circuit breakers (on/off) can assist the fault location algorithms.

Many algorithms have been developed to find the location of fault accurately. There are

four main categories for fault location methods: method using current and voltage waveforms' fundamental frequency components, method using current and voltage waveforms' high frequency components, method using travelling waves created by fault and knowledge based methods such as neural networks, fuzzy logics, genetic algorithms, etc.[8].

In [8], the author described fault location method using measurements of fundamental frequency current and voltage at one terminal of the line. This method considers circuit model of line before and during fault to formulate the calculation of distance from fault to one line terminal. Figure 4.1 is the circuit diagram of faulted line. Using Kirchhoff's law, the relation between current and voltage measured at terminal A and fault current is:

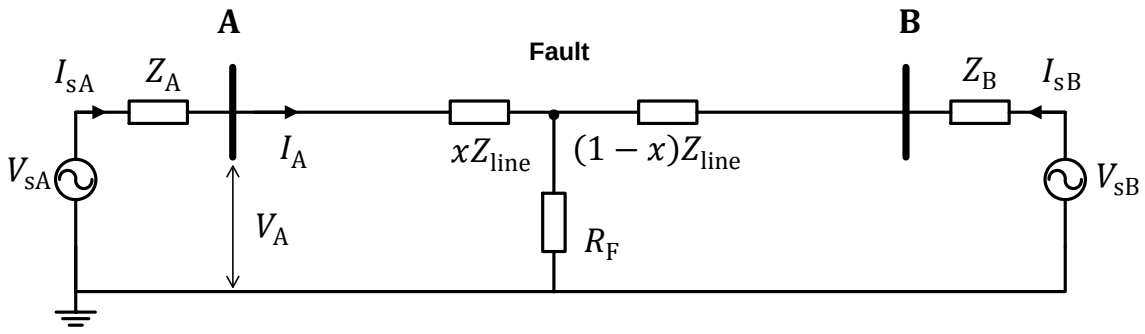


Figure 4.1: Circuit diagram of faulted line

$$V_A = xZ_{line}I_A + R_F I_F \tag{4.1}$$

Fault current distribution factor is defined as:

$$k_F = |k_F|e^{j\gamma} = \frac{(1-x)Z_{line} + Z_B}{Z_A + Z_{line} + Z_B} \tag{4.2}$$

Fault current can be calculated using fault current distribution factor:

$$I_{\mathrm{F}} = \frac{\Delta I_{\mathrm{A}}}{k_{\mathrm{F}}} \tag{4.3}$$

Substitute (4.3) to (4.1)

$$V_{\mathrm{A}} - xZ_{\mathrm{line}}I_{\mathrm{A}} - R_{\mathrm{F}}\frac{\Delta I_{\mathrm{A}}}{|k_{\mathrm{F}}|e^{j\gamma}} = 0 \tag{4.4}$$

(4.4) is equivalent to:

$$V_{\mathrm{A}}e^{j\gamma}\Delta I_{\mathrm{A}}^{*} - xZ_{\mathrm{line}}I_{\mathrm{A}}e^{j\gamma}\Delta I_{\mathrm{A}}^{*} - R_{\mathrm{F}}\frac{|\Delta I_{\mathrm{A}}|^{2}}{|k_{\mathrm{F}}|} = 0 \tag{4.5}$$

Since $R_{\mathrm{F}}\frac{|\Delta I_{\mathrm{A}}|^{2}}{|k_{\mathrm{F}}|}$ is real number, the location of fault is found by taking the imaginary part of (4.5). Assuming the fault current distribution factor is a real number, fault location can be determined without knowing source impedances $Z_{\mathrm{A}}$ and $Z_{\mathrm{B}}$.

$$x = \frac{\mathrm{Im}\left(V_{\mathrm{A}}e^{j\gamma}\Delta I_{\mathrm{A}}^{*}\right)}{\mathrm{Im}\left(Z_{\mathrm{line}}I_{\mathrm{A}}e^{j\gamma}\Delta I_{\mathrm{A}}^{*}\right)} \tag{4.6}$$

This method is simple and can locate the fault with low resolution measurements. However, the accuracy of this method decreases when fault current distribution factor is not a real number. Also, if the fault is clear after a very short time, this method may not be able to locate fault accurately.

In [17], fault is located by precisely determined the arriving time of voltage or current travelling waves. Assuming the resistance of transmission line is negligible, voltage and current are described by partial differential equations:

$$\frac{\partial v(x,t)}{\partial x} = -L\frac{\partial i(x,t)}{\partial t} \tag{4.7}$$

$$\frac{\partial i(x,t)}{\partial x} = -C\frac{\partial v(x,t)}{\partial t} \tag{4.8}$$

Using the above partial different equations, both voltage are current are derived as combination of two travelling waves which propagate in opposite directions.

$$v(x,t) = v^{+}\left(t - \frac{x}{\nu}\right) + v^{-}\left(t + \frac{x}{\nu}\right) \tag{4.9}$$

$$i(x,t) = \frac{1}{Z_c}\left[v^{+}\left(t - \frac{x}{\nu}\right) - v^{-}\left(t + \frac{x}{\nu}\right)\right] \tag{4.10}$$

where $\nu = \frac{1}{\sqrt{LC}}$ is the velocity of propagation and $Z_c = \sqrt{L/C}$ is the characteristic impedance or surge impedance.

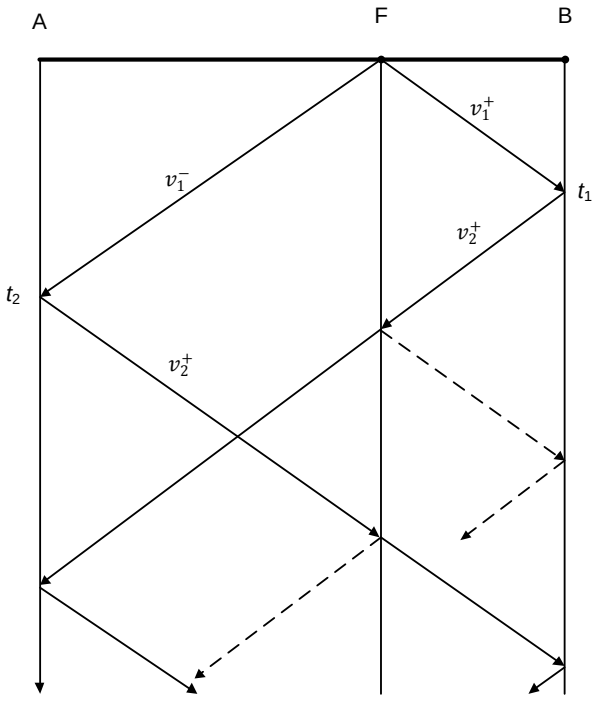


Figure 4.2: Lattice diagram for fault on transmission line

When a fault occurs in a transmission lines, it generates voltage and current transient waves. From the fault location, these transient waves travel toward two terminals of the line. The reflection and refraction of travelling waves that occurs during the fault

transient are illustrated by lattice diagram in Figure 4.2.

The arriving time of transient waves at two terminals are $t_1$ and $t_2$. Knowing the time difference, the line's length and the velocity of wave propagation $v = \frac{1}{\sqrt{LC}}$ , the distance from fault location to bus A can be determined.

$$x = \frac{l - v\Delta t}{2} \tag{4.11}$$

High frequency components of voltage and current transients can be used for fault location. One of the techniques to analyze a transient waveform in frequency domain is using Fourier transform (4.12).

$$S(\omega) = \frac{1}{2\pi}\int_{-\infty}^{+\infty} s(t)e^{-j\omega t}dt \tag{4.12}$$

The author of [18] describes the way voltage waveforms are used to locate fault. Voltage waveforms at two terminals in a selected time interval that fault occurs are extracted from original waveforms. The transient components are then obtained by eliminating the fundamental frequency components (60Hz). After this step is accomplished, transient waveform are analyzed by Leon Cohen time frequency distribution. This step can be done by Fourier transform as well. However, time frequency technique shows a more accurate characterization of transient waveforms.

$$C_s(t,\omega,\phi) = \frac{1}{4\pi^2}\iiint s^*\left(u - \frac{\tau}{2}\right)s\left(u + \frac{\tau}{2}\right)\phi(\theta,\tau)e^{-j\theta t - j\tau\omega + j\theta u}d\theta d\tau du \tag{4.13}$$

Transient waveforms of voltages at two terminals of the line have highest magnitudes at frequencies $\omega_1$ and $\omega_2$. Using (3.13), $\omega_1$ and $\omega_2$ can be determined. Location of fault is then calculated by:

$$x = \frac{L}{1 + \frac{\omega_1}{\omega_2}} \tag{4.14}$$

The limitation of methods using waveforms' high frequency components or travelling waves is the requirement of high sampling rate and the availability of communication.

## 4.2. NETWORK IMPEDANCE MATRIX CALCULATION

When a fault happened, network impedance matrix changed. According to [19], the change that a fault makes in a network can be considered as combination of four basic cases:

- (1) Add branch from a new bus to ground
- (2) Add a branch connect an existing bus to a new bus
- (3) Add a branch from an existing bus to ground
- (4) Add/remove a branch between two existing buses

When a branch with impedance *z* is added from a new bus *N+1* to ground, the new network impedance matrix is calculated as:

$$\underline{\boldsymbol{Z}}_{\boldsymbol{new}} = \begin{bmatrix} & \underline{\boldsymbol{Z}} & & 0 \\ & & & \dots \\ & & & 0 \\ 0 & \dots & 0 & z \end{bmatrix} \tag{4.15}$$

When a branch with impedance z is added to connect an existing bus p to a new bus N+1, the new network impedance matrix is calculated by equation:

$$\underline{\mathrm{Z}}_{\mathrm{new}} = \begin{bmatrix} & & & \mathrm{Z}_{1\mathrm{p}} \\ & \underline{\mathrm{Z}} & & \dots \\ & & & \mathrm{Z}_{\mathrm{Np}} \\ \mathrm{Z}_{\mathrm{p1}} & \dots & \mathrm{Z}_{\mathrm{pN}} & \mathrm{Z}_{1\mathrm{p}} + \mathrm{z} \end{bmatrix} \tag{4.16}$$

When a branch with impedance z is added from an existing bus p to ground, the new network impedance matrix is calculated by two steps. The first step is to add a branch with impedance z to a new bus N+1 using the method of case (2). The second step is to short the new bus N+1 to ground using Kron reduction. New network impedance matrix has the same size as pre-fault network impedance matrix and is calculated by equations (4.17) and (4.18).

$$\underline{Z}^1 = \begin{bmatrix} & & & \mathrm{Z_{1p}} \\ & \underline{\mathrm{Z}} & & \dots \\ & & & \mathrm{Z_{Np}} \\ \mathrm{Z_{p1}} & \dots & \mathrm{Z_{pN}} & \mathrm{Z_{1p}} + \mathrm{z} \end{bmatrix} \tag{4.17}$$

$$Z_{ij}^{new} = Z_{ij}^1 - \left(Z_{i,N+1}^1 Z_{N+1,j}^1\right)/Z_{N+1,N+1}^1 \tag{4.18}$$

Similar to the case (3), calculation of network impedance matrix when a branch with impedance $z$ is added to connect two existing buses $p$ and $q$ includes two steps. First, matrix $\boldsymbol{\underline{Z}^1}$ is calculated to represent the new loop. Then Kron reduction was used to calculate the network impedance matrix of new network.

$$\underline{Z}^1 = \begin{bmatrix} & & & \left(Z_{1p} - Z_{1q}\right) \\ & \underline{\mathrm{Z}} & & \dots \\ & & & \left(Z_{pN} - Z_{qN}\right) \\ \left(Z_{p1} - Z_{q1}\right) & \dots & \left(Z_{pN} - Z_{qN}\right) & Z_{pp} + Z_{qp} - Z_{pq} - Z_{qp} + \mathrm{z} \end{bmatrix} \tag{4.19}$$

$$Z_{ij}^{new} = Z_{ij}^1 - \left(Z_{i,N+1}^1 Z_{N+1,j}^1\right)/Z_{N+1,N+1}^1 \tag{4.20}$$

Equations (4.19) to (4.20) are calculation of network impedance matrix when a branch is added to the network but they can also be used when a branch is removed. In that case, removing a branch with impedance z can be consider as adding a branch with impedance –z.

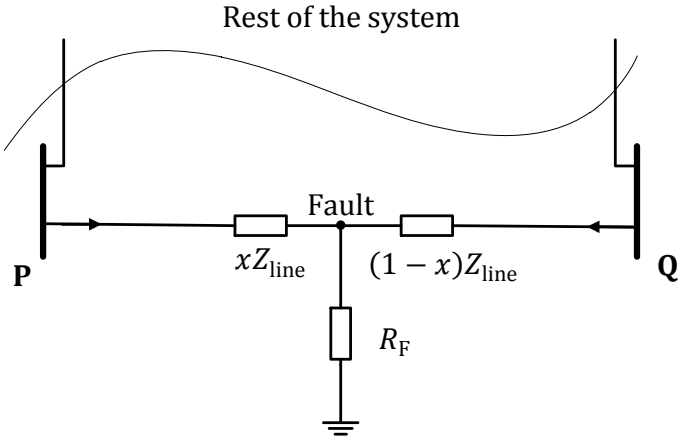


Figure 4.3: Faulted line

Both open circuit and short circuit event can be calculated using these above basic cases in combination. Some scenarios will be considered in this section.

Figure 4.3 is the scenario when three phase fault occurs in transmission line between bus $p$ and bus $q$ of the network. The distance from fault location to bus p is represented by variable $x$ $(0 \leq x \leq 1)$. $x = 0$ when fault occurs at bus $p$ and $x = 1$ when fault occurs at bus $q$. The resistance of fault is $R_F$.

Before fault occurs, impedance matrix of the system is $\underline{\boldsymbol{Z}}$. Impedance of the transmission line is $Z_{line}$. The number of nodes is $N$. The new network during fault shown in Figure 4.3 can be built by the following steps:

- Remove the branch between two existing buses $p$ and $q$
- Add a branch with impedance $xZ_{line}$ from bus $p$ to new bus $N+1$
- Add a branch with impedance $(1-x)Z_{line}$ from bus $q$ to bus $N+1$
- Add a branch with impedance $R_F$ connecting bus $N+1$ to ground

As the result, the network impedance during fault is calculated by the following equations:

$$\underline{\boldsymbol{Z}}^{\mathbf{1}} = \begin{bmatrix} & \underline{\mathrm{Z}} & \begin{matrix} (Z_{1p} - Z_{1q}) \\ \dots \\ (Z_{pN} - Z_{qN}) \end{matrix} \\ (Z_{p1} - Z_{q1}) & \dots \; (Z_{pN} - Z_{qN}) & Z_{pp} + Z_{qp} - Z_{pq} - Z_{qp} - Z_{line} \end{bmatrix} \tag{4.21}$$

$$Z_{ij}^{2} = Z_{ij}^{1} - \left(Z_{i,N+1}^{1} Z_{N+1,j}^{1}\right) / Z_{N+1,N+1}^{1} \tag{4.22}$$

$$\underline{\boldsymbol{Z}}^{\mathbf{3}} = \begin{bmatrix} & \underline{\boldsymbol{Z}}^{\mathbf{2}} & \begin{matrix} Z_{1p}^{2} \\ \dots \\ Z_{Np}^{2} \end{matrix} \\ Z_{1p}^{2} & \dots \; Z_{1p}^{2} & Z_{1p}^{2} + xZ_{line} \end{bmatrix} \tag{4.23}$$

$$\underline{\boldsymbol{Z}}^{\mathbf{4}} = \begin{bmatrix} & \underline{\boldsymbol{Z}}^{\mathbf{3}} & \begin{matrix} (Z_{1p}^{3} - Z_{1q}^{3}) \\ \dots \\ (Z_{p(N+1)}^{3} - Z_{q(N+1)}^{3}) \end{matrix} \\ (Z_{p1}^{3} - Z_{q1}^{3}) & \dots \; (Z_{p(N+1)}^{3} - Z_{q(N+1)}^{3}) & \begin{matrix} Z_{pp}^{3} + Z_{qq}^{3} - Z_{qp}^{3} - \\ -Z_{pq}^{3} + (1-x)Z_{line} \end{matrix} \end{bmatrix} \tag{4.24}$$

$$Z_{ij}^{5} = Z_{ij}^{4} - \left(Z_{i,N+2}^{4} Z_{N+2,j}^{4}\right) / Z_{N+2,N+2}^{4} \tag{4.25}$$

$$\underline{\boldsymbol{Z}}^{\mathbf{6}} = \begin{bmatrix} & \underline{\boldsymbol{Z}}^{\mathbf{5}} & \begin{matrix} Z_{1p}^{5} \\ \dots \\ Z_{(N+1)p}^{5} \end{matrix} \\ Z_{p1}^{\mathbf{5}} & \dots \; Z_{p(N+1)}^{\mathbf{5}} & Z_{1p}^{\mathbf{5}} + R_F \end{bmatrix} \tag{4.26}$$

$$Z_{ij}^{F} = Z_{ij}^{6} - \left(Z_{i,N+1}^{6} Z_{N+2,j}^{6}\right) / Z_{N+2,N+2}^{6} \tag{4.27}$$

From (4.21) to (4.27), $Z_{ij}^{k}$ is the element of impedance matrix $\underline{\boldsymbol{Z}}^{k}$ at row $i$ and column $j$. $\underline{\boldsymbol{Z}}^{F}$ is the impedance matrix of faulted system.

Now, we consider the transmission line with two circuit breakers at bus p and bus q. If the setting of two circuit breakers is different or the location of fault is closer to on bus

than the other bus, one circuit breaker will trip before the other. Figure 4.2 shows the network when the circuit breaker at Q bus trips during fault. The new network impedance matrix can be built by these steps below:

- Remove the branch between two existing buses *p* and *q*

- Add a branch with impedance $xZ_{line}$ from bus p to new bus N+1

- Add a branch with impedance $R_F$ connecting bus N+1 to ground

As the result, the network impedance during fault is calculated by the following equations:

$$\underline{\boldsymbol{Z}}^{\boldsymbol{1}} = \begin{bmatrix} & \underline{\mathrm{Z}} & \begin{matrix}(Z_{1p}-Z_{1q})\\ \dots \\ (Z_{pN}-Z_{qN})\end{matrix} \\ (Z_{p1}-Z_{q1}) & \dots \quad (Z_{pN}-Z_{qN}) & Z_{pp}+Z_{qp}-Z_{pq}-Z_{qp}-Z_{line} \end{bmatrix} \tag{4.28}$$

$$Z_{ij}^{2} = Z_{ij}^{1} - \left(Z_{i,N+1}^{1} Z_{N+1,j}^{1}\right)/Z_{N+1,N+1}^{1} \tag{4.29}$$

$$\underline{\boldsymbol{Z}}^{\boldsymbol{3}} = \begin{bmatrix} & \underline{\boldsymbol{Z}}^{\boldsymbol{2}} & \begin{matrix}Z_{1p}^{2}\\ \dots \\ Z_{Np}^{2}\end{matrix} \\ Z_{1p}^{2} & \dots \quad Z_{1p}^{2} & Z_{1p}^{2}+xZ_{line} \end{bmatrix} \tag{4.30}$$

$$\underline{\boldsymbol{Z}}^{\boldsymbol{4}} = \begin{bmatrix} & \underline{\boldsymbol{Z}}^{\boldsymbol{3}} & \begin{matrix}Z_{1p}^{3}\\ \dots \\ Z_{(N+1)p}^{3}\end{matrix} \\ \boldsymbol{Z_{p1}^{3}} & \dots \quad \boldsymbol{Z_{p(N+1)}^{3}} & \boldsymbol{Z_{1p}^{3}} + R_F \end{bmatrix} \tag{4.31}$$

$$Z_{ij}^{F} = Z_{ij}^{4} - \left(Z_{i,N+1}^{4} Z_{N+2,j}^{4}\right)/Z_{N+2,N+2}^{4} \tag{4.32}$$

Another scenario is when both circuit breaker at two ends of the transmission line trip.

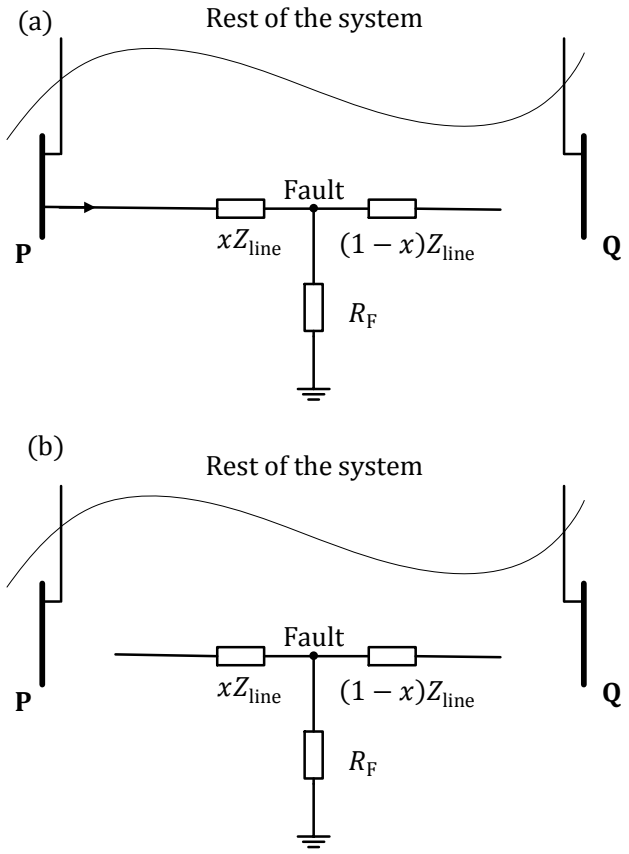


Figure 4.4: Faulted system

(a) with one circuit breaker open and (b) with two circuit breaker open

For this scenario, the new network impedance matrix can be calculated by simply removing the branch between bus p and bus q. We will also have the same network for the case of open fault in transmission line between bus p and q, assuming the line is inductive and its capacitance can be neglected.

$$\underline{\boldsymbol{Z}}^{\mathbf{1}} = \begin{bmatrix} & \underline{\mathrm{Z}} & \begin{matrix} (Z_{1p} - Z_{1q}) \\ \dots \\ (Z_{pN} - Z_{qN}) \end{matrix} \\ (Z_{p1} - Z_{q1}) & \dots \; (Z_{pN} - Z_{qN}) & Z_{pp} + Z_{qp} - Z_{pq} - Z_{qp} - Z_{line} \end{bmatrix} \tag{4.33}$$

$$Z_{ij}^{F} = Z_{ij}^{1} - \left(Z_{i,N+1}^{1} Z_{N+1,j}^{1}\right) / Z_{N+1,N+1}^{1} \tag{4.34}$$

## 4.3. FINDING FAULT AS A NON-LINEAR LEAST SQUARES PROBLEM

### 4.3.1. LEAST SQUARES

A common problem in engineering is to find parameters of a device or process with some available measurements. The relation between these parameters that need to be estimated and the measured variables is known from theoretical study of the object. In many cases, this problem is over-defined, for example when measurements are taken multiple times. Least squares method is an approach to solve over-defined equations where the number of variables is less than the number of equations. Because of the redundancy, in general case, there is no set of variables that satisfy the system of equations. Least square method finds the approximate solution that minimizes quadratic mean of errors made in each equation.

Suppose the relations between unknown variables and measurements are provided as a set of linear equations:

$$AX = Y \tag{4.35}$$

with $A$ is a matrix that have more rows than columns, $Y$ is a matrix with one column, $X$ is the variable. The linear least squares problem is to find solution $\hat{X}$ to minimize error $\varepsilon = \left\| Y - A\hat{X} \right\|$.

This is an optimization problem. The solution is

$$\hat{X} = (A^T A)^{-1} A^T Y \tag{4.36}$$

Least squares approach is useful in data fitting application. Figure 4.5 is a data fitting

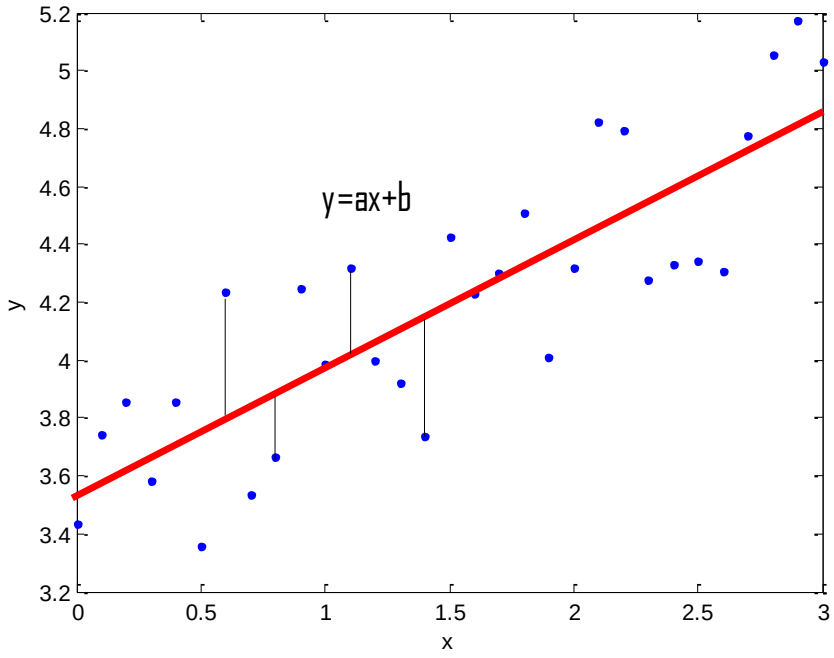


Figure 4.5: Data fitting using linear least square

problem that can be solved using least squares. Measurements are taken multiple times at different points and with each measurement, we have one equation. The set of equations obtained is:

$$\begin{cases} 0.1a + b = 3.74 \\ 0.2a + b = 3.85 \\ 0.3a + b = 3.58 \\ \quad\quad ... \\ 3a + b = 5.03 \end{cases} \tag{4.37}$$

(4.37) can be expressed in the matrix form (4.35) with

$$A = \begin{bmatrix} 0.1 & 1 \\ 0.2 & 1 \\ 0.3 & 1 \\ ... & ... \\ 3 & 1 \end{bmatrix}; \mathrm{X} = \begin{bmatrix} a \\ b \end{bmatrix}; Y = \begin{bmatrix} 3.74 \\ 3.85 \\ 3.58 \\ ... \\ 5.03 \end{bmatrix} \tag{4.38}$$

$$\hat{X} = (A^T A)^{-1} A^T Y = \begin{bmatrix} 0.4624 \\ 3.6339 \end{bmatrix} \tag{4.39}$$

That means the line in Figure 4.5 is $y = 0.4624x + 3.6339$.

### 4.3.2. NON-LINEAR LEAST SQUARES

When the relation between unknown variables and measurements is non-linear, equation has the form:

$$f(X) = 0 \tag{4.40}$$

Similar to the case of linear least square, solution $\hat{X}$ has to minimize quadratic mean error $\varepsilon = \|f(\hat{X})\|$.

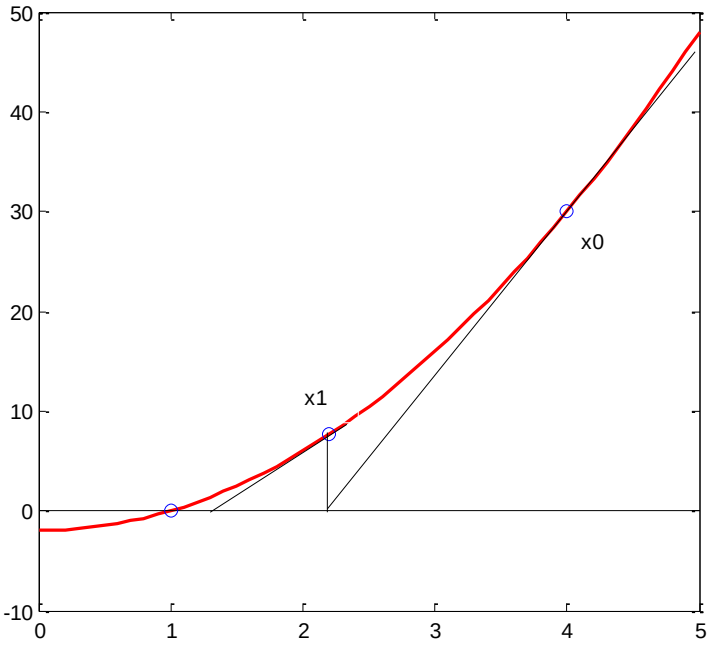


Figure 4.6: Solving non-linear equations

As a non-linear equation, (4.40) can be solved using iteration. However, because it is redundant, each steps of the iteration is solved using linear least square. The iteration process is described in Figure 4.6.

The iteration starts at $X_0$. If variable $X$ is has one dimension only, the equation of tangent line is:

$$\frac{df(X)}{dX}_{|X=X_0}(X - X_0) = Y - f(X_0) \tag{4.41}$$

Then the first step of the iteration is to find $X_1$ where tangent line (4.41) cuts horizontal axis ($Y = 0$).

$$\frac{df(X)}{dX}_{|X=X_0}(X - X_0) = -f(X_0) \tag{4.42}$$

Equation (4.42) can be solved by linear least square method (4.36):

$$X_1 = X_0 - (H^T H)^{-1} H^T f(X_0) \tag{4.43}$$

with $H = \frac{df(X)}{dX}_{|X=X_0}$. When $X$ has more than one dimension $X = (x_1, x_2, \dots, x_n)$, H is a matrix of first partial derivatives of function $f(X)$:

$$H = \begin{bmatrix} \frac{df}{dx_1}_{|X=X_0} & \frac{df}{dx_2}_{|X=X_0} & \cdots & \frac{df}{dx_n}_{|X=X_0} \end{bmatrix} \tag{4.44}$$

Notice that function $f$ may have more than one dimension so matrix H can have more than one row.

For example, for the equation

$$\begin{bmatrix} x_1^2 - 4x_2 + 4 \\ 3x_1 + x_2^2 - 1 \\ 3x_1 + 1.01x_2^2 - 1 \end{bmatrix} = \begin{bmatrix} 0 \\ 0 \\ 0 \end{bmatrix} \tag{4.45}$$

The matrix H is calculated by:

$$H = \begin{bmatrix} 2x_1 & -4 \\ 3 & 2x_2 \\ 3 & 2.02x_2 \end{bmatrix}_{|x_1=x_1^0, x_2=x_2^0} \quad (4.46)$$

After the solution $X_1$ of (4.43) is found then assign $X_0 = X_1$ and repeat the process until the incremental error is small enough $\|X_0 = X_1\| \leq \varepsilon$.

### 4.3.3. FINDING FAULT LOCATION

Consider the location of fault x ($0 \leq x \leq 1$) and fault resistance $R_F$ are unknown variables, the network impedance matrix during fault can be calculated as a function of ($x$, $R_F$) by equations (4.21) to (4.27). Then the voltages at all nodes in the network can be calculated as a function of ($x$, $R_F$) as well:

$$\begin{bmatrix} V_1 \\ V_2 \\ \dots \\ V_N \end{bmatrix} = \underline{\boldsymbol{Z}} \begin{bmatrix} I_{g1} \\ I_{g2} \\ \dots \\ I_{gN} \end{bmatrix} \quad (4.47)$$

with $I_{gi}$ is current injected to bus $i$.

Currents at all lines in the network then can be calculated from bus voltages and line impedance data. As a result both bus voltages $V_i$ and line currents $I_{ij}$ can be calculated as function of ($x$, $R_F$):

$$V_i = f_i(x, R_F) \quad (4.48)$$

$$I_{jk} = g_{jk}(x, R_F) \quad (4.49)$$

Consider the network that we have voltage phasor measurements at buses $i_1, i_2, \dots, i_n$ and current phasor measurement at lines $j_1k_1, j_2k_2, \dots, j_mk_m$

Equation:

$$\begin{bmatrix} f_{i_1}(x,\ R_F) \\ f_{i_2}(x,\ R_F) \\ \cdots \\ f_{i_n}(x,\ R_F) \\ g_{j_1k_1}(x,\ R_F) \\ g_{j_2k_2}(x,\ R_F) \\ \cdots \\ g_{j_mk_m}(x,\ R_F) \end{bmatrix} - \begin{bmatrix} V_{i_1} \\ V_{i_2} \\ \cdots \\ V_{i_n} \\ I_{j_1k_1} \\ I_{j_1k_1} \\ \cdots \\ I_{j_mk_m} \end{bmatrix} = 0 \tag{4.50}$$

(4.50) is the set of $m+n$ equation with 2 variables. Using non-linear least square method discussed in section 4.3.2 we can find location of fault $x$ and fault resistance $R_F$.

# CHAPTER 5

## TEST CASES IN PSCAD AND RESULT

In this chapter, fault location method described in chapter 4 is applied to locate fault in three test cases: 6 bus network case, single circuit line case and double circuit lines case. For the 6 bus network case, the fault locator uses model of the of the system and measurement data obtained from simulation. For the single circuit line case and double circuit lines case, the system model is estimated from voltage and current measurements, then this model is used to locate fault. All three test cases are simulated in PSCAD.

## 5.1. 6 BUS NETWORK CASE

### 5.1.1. SYSTEM DESCRIPTION

The 6 bus system in has two voltage sources and four loads at bus 2, 3, 4 and 5. Voltage level is 169 kV. Pre-fault system is described in Table 5.1,

Table 5.2 and Table 5.3 . As the length of transmission line is short, line capacitance is neglected in this test case.

The simulated scenario is a three phase ground fault. Fault occurs in transmission line that connects bus 4 and bus 5. Location of fault is 125 km from bus 4 which is equal to 85% of total length of the line. The duration of fault is 0.5 s and after fault is clear, the system is back to normal operation. The fault resistance is 50 Ohm.

In this simulation, circuit breaker is not included. That means the network topology

doesn't change during the fault. Instantaneous voltages of bus 1 and bus 5 and instantaneous currents of line 1-2 and line 5-3 are measured.

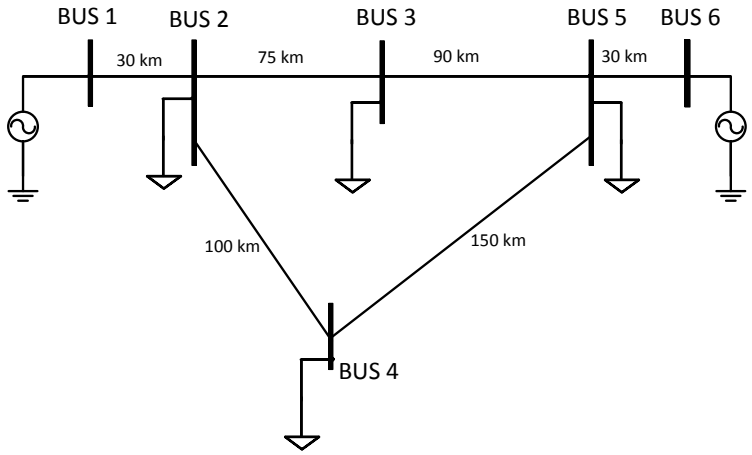


Figure 5.1: 6 bus system

Table 5.1: Voltage sources in 6 bus system

| Voltage source at bus | Magnitude (kV) | Angle (Degree) |
|---|---|---|
| 1 | 164.22 | 1.91 |
| 6 | 164.22 | 0 |

Table 5.2: Load in 6 bus system

| Load at bus | Real power (MW) | Reactive power (MVAR) |
|---|---|---|
| 2 | 20 | 4 |
| 3 | 100 | 5 |
| 4 | 10 | 30 |
| 5 | 10 | 2 |

Table 5.3: Line parameters

| Line | Length (km) | Resistance (Ohm) | Inductance (Ohm) |
|---|---|---|---|
| 1-2 | 30 | 1.5864 | 12.887 |
| 2-3 | 75 | 3.9659 | 32.2175 |
| 2-4 | 100 | 5.2879 | 42.9567 |
| 3-5 | 90 | 4.7591 | 38.6610 |
| 4-5 | 150 | 7.9318 | 64.4351 |
| 5-6 | 30 | 1.5864 | 12.8870 |

### 5.1.2. RESULT

The three phase ground fault described in section 5.1.1 is simulated in PSCAD. Three phase instantaneous voltages and currents are measured and imported to MATLAB. Figure 5.2 is a close look of instantaneous current in line 1 – 2 at the moment fault occurs. The increase of current magnitude indicates that the fault is fed from power source at bus 1.

After instantaneous voltages and currents from PSCAD are imported to MATLAB, they will be processed by the phasor measurement algorithm mentioned in chapter 2. Positive sequence voltage and current phasors are estimated. Because a phasor has complex value, we will have phasor magnitude and phase angle. These magnitude and phase angle of our selected voltage and current change as the fault occurs.

Figure 5.3 and Figure 5.4 show that there are both changes in current magnitude and phase angle. For voltage phasor, only voltage at bus 5 changes when fault occurs.

Voltage at bus 1 doesn't change because the power source used in this simulation is ideal.

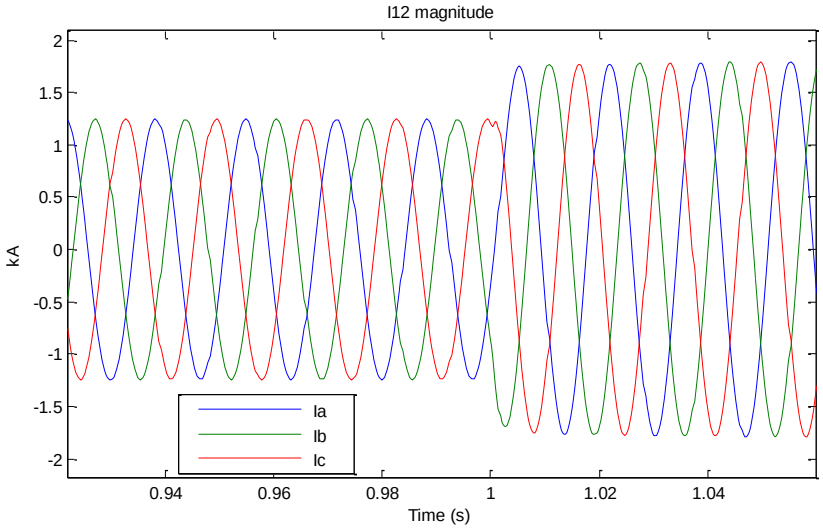


Figure 5.2: Instantaneous current in line 1 – 2

This observation shows that current phasor is more sensitive to fault and it will be useful to use current magnitude, current phase angle or both of them to detect the fault. Certainly, for the case fault impedance is high, the change of current magnitude and phase angle will be small and as a result, a specified detection method for high impedance fault detection will need to be used. This issue however is not covered in the scope of this thesis.

In Figure 5.3 and Figure 5.4, red dots indicate the selected moment which faulted line is connecting to ground through a resistance. In this case, the moment is $t_1 = 1.5$ s. $t_1$ is selected so that the system has reached steady state and both circuit breakers are closed. The fault locator can select this moment by looking at the change in magnitude and phase angle of current phasors. Also, the state of circuit breakers can be used to improve the accuracy of the fault location algorithm if there is communication between circuit breakers and the operation center.

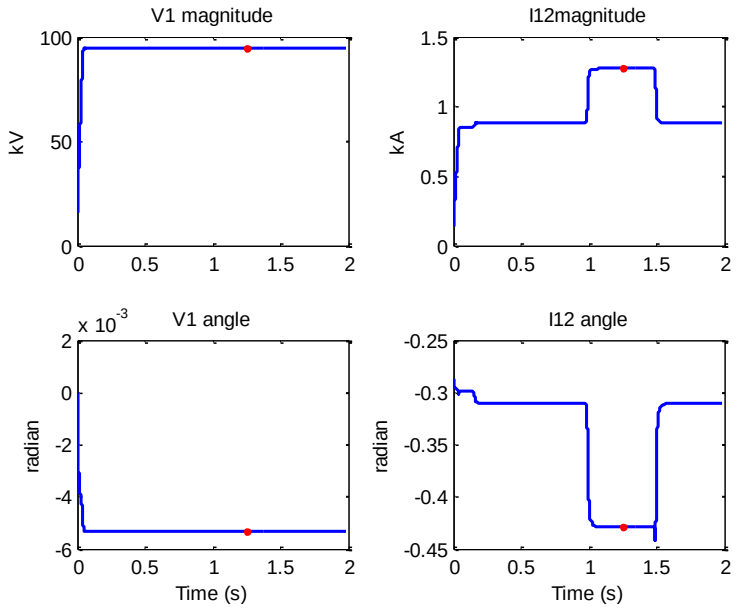


Figure 5.3: Voltage and current phasors at bus 1

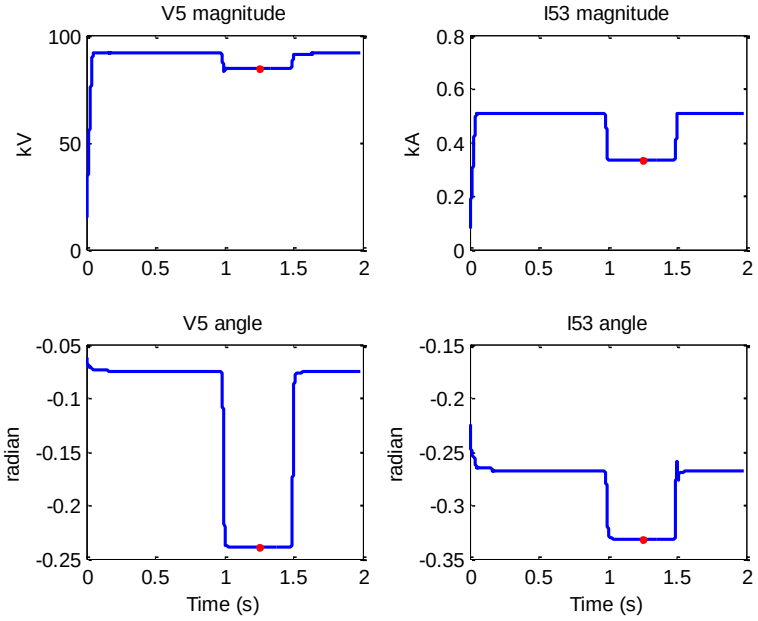


Figure 5.4: Voltage and current phasors at bus 5

In practice, it can happen that two circuit breakers at two ends of the faulted line trips quickly after the moment fault occur. From chapter 2, we have concluded that the phasor

estimation is reliable only when the data window of the signal is in steady state. Hence, if the circuit breakers trips before 1 cycle of steady state voltage and current waveforms are collected, the estimation will not be accurate. In this case, transient monitoring function can be used to in the selection of $t_1$.

At moment $t_1$ we have measured value of voltages at bus 1 and bus 5 and currents in line 1 – 2 and line 5 – 3 ($V_1, V_5, I_{12}, I_{53}$). From (4.48) (4.49) and (4.50), these values can be calculated from system's model as a function of fault location and fault resistance, with assumption that fault occurs on a particular line:

$$V_i = f_i(x,\ R_F) \tag{5.1}$$

$$I_{jk} = g_{jk}(x,\ R_F) \tag{5.2}$$

The equation with variable $x$ and $R_F$:

$$\begin{bmatrix} f_1(x,\ R_F) \\ f_5(x,\ R_F) \\ g_{12}(x,\ R_F) \\ g_{53}(x,\ R_F) \end{bmatrix} - \begin{bmatrix} V_1 \\ V_5 \\ I_{12} \\ I_{53} \end{bmatrix} = 0 \tag{5.3}$$

Table 5.4 is the solutions for fault location and fault resistance.

In Table 5.4, N/A means the iteration process to solve (5.3) doesn't converge or the solution found is out of boundary. The constraints for fault location and fault resistance are $0 \leq x \leq 1$ and $R_F \geq 0$. E is the absolute value of the left side of equation (5.3).

With assumption that fault occurs on line 3-5, the iteration process converses to the point $x = 80.96\%$ and $R_F = 46$ Ohm. Suppose fault occurs on line 3-5, the iteration process converses to the point $x = 85.6\%$ and $R_F = 46.4$ Ohm. Now, the error E is considered. The latter solution $R_F = 46.4$ Ohm and $x = 85.6\%$ on line 4 – 5 is the final

answer because it minimizes the absolute value of the left side of equation (5.3).

Table 5.4: Fault location and fault resistance

| Assume fault occurs on line | Fault location (%) | Fault Resistance (Ohm) | Error |
|---|---|---|---|
| 1-2 | N/A | N/A | |
| 2-3 | N/A | N/A | |
| 2-4 | N/A | N/A | |
| 3-5 | 80.96 | 46 | 2.8551 |
| 4-5 | 85.6 | 46.4 | 0.8779 |
| 5-6 | N/A | N/A | |

Table 5.5: 6 bus system fault location result

| Faulted line | Location of fault | Error in percentage of line length |
|---|---|---|
| 1-2 | 85.6 % | 0.4 % |

## 5.2. SINGLE CIRCUIT LINE CASE

Single circuit line is the simplest case of the fault location problem. Now, the fault locator receives available measurements from this line and uses these data to detect if fault occurs and the location of fault on this line. The system consists of the line that fault locator is monitoring and the outside network. The impedance of the line can be estimated from the line length and cable type. The outside network is unknown. Fortunately, assuming the linearity of the network, it can be equivalence to a two bus

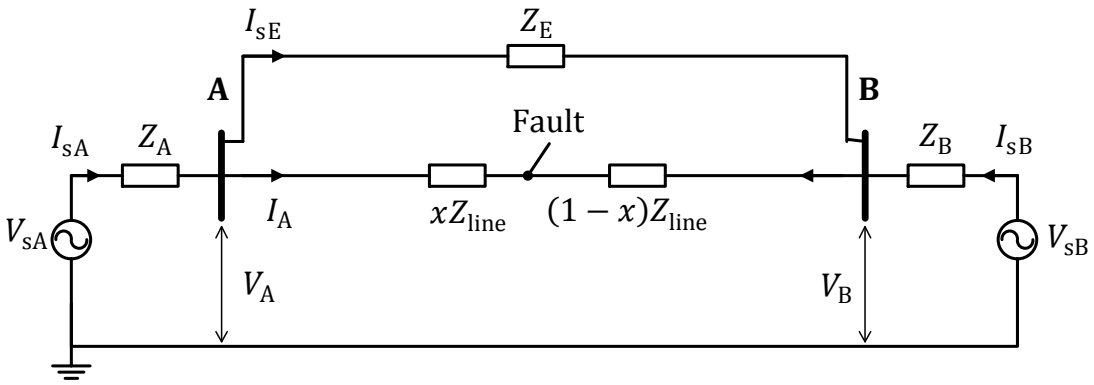


Figure 5.5: Single circuit case

system with an extra link line.

Figure 5.5 is the equivalent model of the single circuit line case. The two terminals of the monitored line are name A and B. The equivalent network consists of two ideal voltage sources $V_{sA}$ and $V_{sB}$ and two source impedance $Z_A$ and $Z_B$. The extra link line with impedance $Z_E$ represents the flow of current from bus A to bus B through the outside network. When $Z_E = 0$, the system becomes two-machine system. In many applications, these values of source impedance are provided for the most typical operations of the system [8]. However, in modern power system with high penetration of distributed power generations and load fluctuations, the provided data may not be accurate. In section 5.2.2, method to obtain the parameters of equivalent model will be discussed.

### 5.2.1. SYSTEM DESCRIPTION

The single circuit line case is simulated in PSCAD and simulation data is imported to Matlab for processing. The system consists of voltage sources and impedances listed in Table 5.6.

Table 5.6: Single circuit line case

| | |
|---|---|
| $V_{sA}$ | $230\angle 0^{o}$ kV L-L |
| $Z_{A}$ | 2+6i Ohm |
| $V_{sB}$ | $207\angle 15^{o}$ kV L-L |
| $Z_{B}$ | 4+12i Ohm |
| $Z_{E}$ | 68+191i Ohm |
| $Z_{line1}$ | 30.7 +93.1i Ohm |

The simulated scenario is a permanent three phase ground fault. Figure 5.5 is the pre-fault system. Location of fault from bus A is 60% of the total line length. Fault occurs at moment $t = 1$s and is kept until the end of simulation. Circuit breakers at two terminals of the line are included in this simulation. The circuit breaker at bus A trips 0.1s after fault occurs and the other circuit breaker at bus B trips at $t = 2.5$s

### 5.2.2. SYSTEM MODELING

First, we consider a branch from bus A or B to ground that has voltage sources $V_{sA}$ and $V_{sB}$, impedance $Z_A$ and $Z_B$. Only bus voltages $V_A, V_B$ and branch current $I_A$ are measured. Suppose there are changes in value of voltage and current overtime due to disturbance in the network, then voltage $V_s$ and impedance $Z$ at each bus can be estimated by equations (5.4) and (5.5):

$$Z = -\frac{\Delta V}{\Delta I_s} \tag{5.4}$$

$$V_s = V + ZI_s \tag{5.5}$$

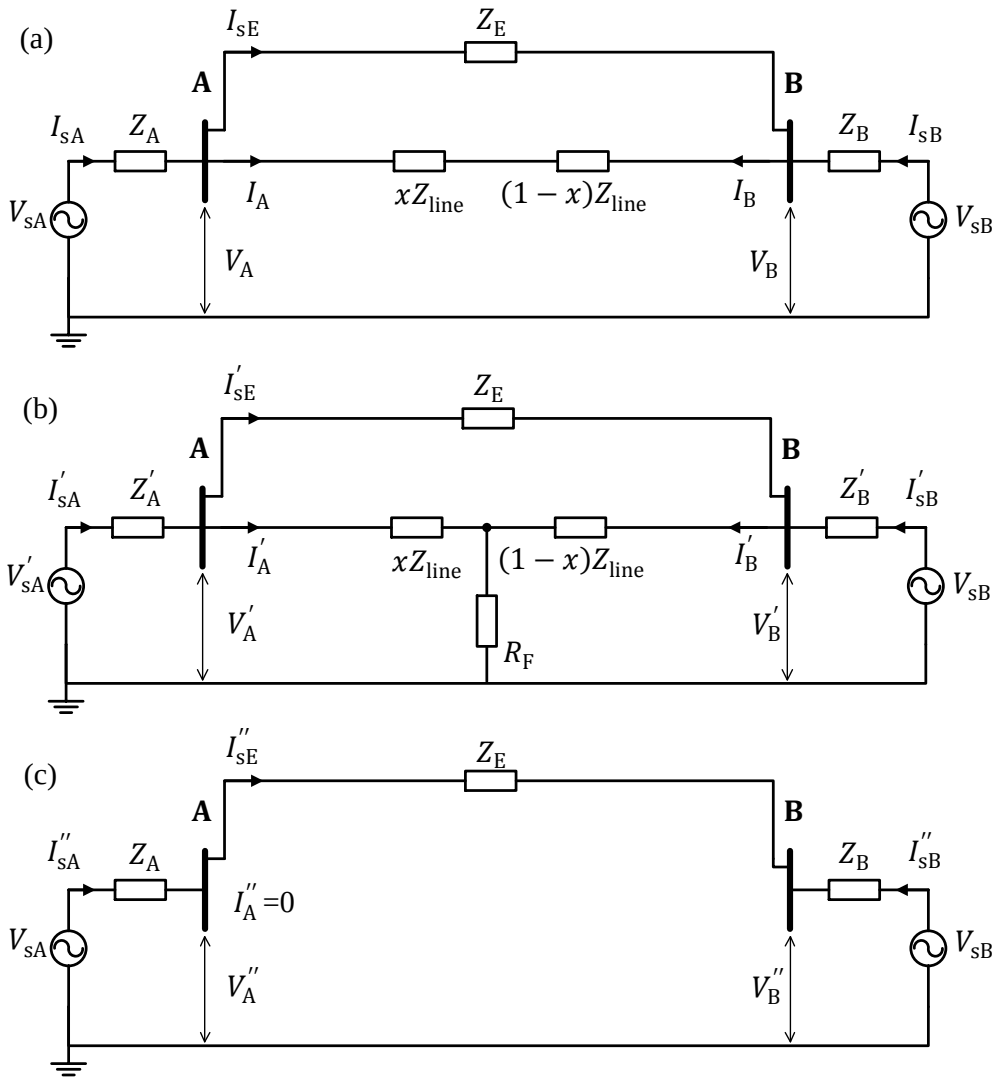


Figure 5.6: Stages of a fault

(a) Pre-fault system, (b) faulted system with two circuit breakers close, and (c) faulted system with circuit breaker at B end opens

Current goes through the extra link in figure can be calculated from bus voltages and line impedance:

$$I_E = \frac{V_A - V_B}{Z_E} \tag{5.6}$$

For network in Figure 5.6, voltages and currents at different stages of a fault are denoted. Pre-fault measurements (at moment $t_1$) are denoted as $V_A, V_B, I_A$ , during fault

when both circuit breakers are closed $V'_{\mathrm{A}}, V'_{\mathrm{B}}, I'_{\mathrm{A}}$ (at moment $t_2$), during fault when one at both circuit breakers is opened $V''_{\mathrm{A}}, V''_{\mathrm{B}}, I''_{\mathrm{A}}$ (at moment $t_3$).

Using (5.4) and (5.5) for bus A and bus B in Figure 5.6, we have:

$$Z_{\mathrm{A}} = -\frac{V'_{\mathrm{A}} - V_{\mathrm{A}}}{I'_{\mathrm{sA}} - I_{\mathrm{sA}}} \tag{5.7}$$

$$V_{\mathrm{sA}} = V_{\mathrm{A}} + Z_{\mathrm{A}} I_{\mathrm{sA}} \tag{5.8}$$

$$Z_{\mathrm{B}} = -\frac{V''_{\mathrm{B}} - V_{\mathrm{B}}}{I''_{\mathrm{sB}} - I_{\mathrm{sB}}} \tag{5.9}$$

$$V_{\mathrm{sB}} = V_{\mathrm{B}} + Z_{\mathrm{B}} I_{\mathrm{sB}} \tag{5.10}$$

Because when both circuit breakers are opened, current flows through impedance $Z_{\mathrm{A}}, Z_{\mathrm{B}}$ and the extra link impedance $Z_{\mathrm{E}}$ are equal.

$$I''_{\mathrm{E}} = I''_{\mathrm{sA}} = I''_{\mathrm{sB}} \tag{5.11}$$

As a result, the current flows through $Z_{\mathrm{E}}$ is:

$$I''_{\mathrm{E}} = \frac{V_{\mathrm{sA}} - V''_{\mathrm{A}}}{Z_{\mathrm{A}}} \tag{5.12}$$

In another the hand, $I''_{\mathrm{E}}$ depends on voltages at two ends of the line and impedance $Z_{\mathrm{E}}$:

$$I''_{\mathrm{E}} = \frac{V''_{\mathrm{A}} - V''_{\mathrm{B}}}{Z_{\mathrm{E}}} \tag{5.13}$$

From equations (5.12) and (5.13), line impedance $Z_{\mathrm{E}}$ is expressed as:

$$Z_{\mathrm{E}} = Z_{\mathrm{A}} \frac{V''_{\mathrm{A}} - V''_{\mathrm{B}}}{V_{\mathrm{sA}} - V''_{\mathrm{A}}} \tag{5.14}$$

Equation (5.7) can be written as

$$Z_{\mathrm{A}} = -\frac{V'_{\mathrm{A}} - V_{\mathrm{A}}}{I'_{\mathrm{A}} - I_{\mathrm{A}} + I'_{\mathrm{E}} - I_{\mathrm{E}}} \tag{5.15}$$

$$Z_{\mathrm{A}} = -\frac{V'_{\mathrm{A}} - V_{\mathrm{A}}}{I'_{\mathrm{A}} - I_{\mathrm{A}} + \dfrac{V'_{\mathrm{A}} - V_{\mathrm{A}} - (V'_{\mathrm{B}} - V_{\mathrm{B}})}{Z_{\mathrm{E}}}} \tag{5.16}$$

From (5.14) and (5.16):

$$Z_{\mathrm{A}} = -\frac{V'_{\mathrm{A}} - V_{\mathrm{A}}}{I'_{\mathrm{A}} - I_{\mathrm{A}} + \dfrac{V'_{\mathrm{A}} - V_{\mathrm{A}} - (V'_{\mathrm{B}} - V_{\mathrm{B}})}{Z_{\mathrm{A}}(V''_{\mathrm{A}} - V''_{\mathrm{B}})}(V_{\mathrm{sA}} - V''_{\mathrm{A}})} \tag{5.17}$$

Equation (5.17) can be re-written as:

$$(I'_{\mathrm{A}} - I_{\mathrm{A}})Z_{\mathrm{A}} + \frac{V'_{\mathrm{A}} - V_{\mathrm{A}} - (V'_{\mathrm{B}} - V_{\mathrm{B}})}{(V''_{\mathrm{A}} - V''_{\mathrm{B}})}V_{\mathrm{sA}} \tag{5.18}$$

$$= \frac{V'_{\mathrm{A}} - V_{\mathrm{A}} - (V'_{\mathrm{B}} - V_{\mathrm{B}})}{(V''_{\mathrm{A}} - V''_{\mathrm{B}})}V''_{\mathrm{A}} - (V'_{\mathrm{A}} - V_{\mathrm{A}})$$

From equation (5.8):

$$V_{\mathrm{sA}} = V_{\mathrm{A}} + Z_{\mathrm{A}}\left(I_{\mathrm{A}} + \frac{V_{\mathrm{A}} - V_{\mathrm{B}}}{Z_{\mathrm{E}}}\right)$$

$$= V_{\mathrm{A}} + Z_{\mathrm{A}}\left(I_{\mathrm{A}} + \frac{V_{\mathrm{A}} - V_{\mathrm{B}}}{Z_{\mathrm{A}}(V''_{\mathrm{A}} - V''_{\mathrm{B}})}(V_{\mathrm{sA}} - V''_{\mathrm{A}})\right) \tag{5.19}$$

Equation (5.19) can be re-written as:

$$I_{\mathrm{A}}Z_{\mathrm{A}} + \left(\frac{V_{\mathrm{A}} - V_{\mathrm{B}}}{(V''_{\mathrm{A}} - V''_{\mathrm{B}})} - 1\right)V_{\mathrm{sA}} = \frac{V_{\mathrm{A}} - V_{\mathrm{B}}}{(V''_{\mathrm{A}} - V''_{\mathrm{B}})}V''_{\mathrm{A}} - V_{\mathrm{A}} \tag{5.20}$$

Now, assign $a_1 = I_{\mathrm{A}}; b_1 = \frac{V_{\mathrm{A}} - V_{\mathrm{B}}}{(V''_{\mathrm{A}} - V''_{\mathrm{B}})} - 1; c_1 = \frac{V_{\mathrm{A}} - V_{\mathrm{B}}}{(V''_{\mathrm{A}} - V''_{\mathrm{B}})}V''_{\mathrm{A}} - V_{\mathrm{A}}$; $a_2 = (I'_{\mathrm{A}} - I_{\mathrm{A}}); b_2 = \frac{V'_{\mathrm{A}} - V_{\mathrm{A}} - (V'_{\mathrm{B}} - V_{\mathrm{B}})}{(V''_{\mathrm{A}} - V''_{\mathrm{B}})}; c_2 = \frac{V'_{\mathrm{A}} - V_{\mathrm{A}} - (V'_{\mathrm{B}} - V_{\mathrm{B}})}{(V''_{\mathrm{A}} - V''_{\mathrm{B}})}V''_{\mathrm{A}} - (V'_{\mathrm{A}} - V_{\mathrm{A}})$; we have a system of two equations with two variables:

$$\begin{cases} a_1 Z_{\mathrm{A}} + b_1 V_{\mathrm{sA}} = c_1 \\ a_2 Z_{\mathrm{A}} + b_2 V_{\mathrm{sA}} = c_2 \end{cases} \tag{5.21}$$

The solution of (5.21) is:

$$\begin{cases} Z_{\mathrm{A}} = \dfrac{c_1 b_2 - c_2 b_1}{a_1 b_2 - a_2 b_1} \\ V_{\mathrm{sA}} = \dfrac{a_1 c_2 - a_2 c_1}{a_1 b_2 - a_2 b_1} \end{cases} \tag{5.22}$$

Impedance $Z_{\mathrm{E}}$ is calculated by substituting (5.22) to (5.14):

$$Z_{\mathrm{E}} = \frac{c_1 b_2 - c_2 b_1}{a_1 b_2 - a_2 b_1} \times \frac{V_{\mathrm{A}}'' - V_{\mathrm{B}}''}{\dfrac{a_1 c_2 - a_2 c_1}{a_1 b_2 - a_2 b_1} - V_{\mathrm{A}}''} \tag{5.23}$$

Substitute (5.23) to (5.9) to calculate $Z_{\mathrm{B}}$:

$$Z_{\mathrm{B}} = -\frac{V_{\mathrm{B}}'' - V_{\mathrm{B}}}{I_{\mathrm{B}}'' - I_{\mathrm{B}} + I_{\mathrm{E}}'' - I_{\mathrm{E}}} \tag{5.24}$$

$$= -\frac{V_{\mathrm{B}}'' - V_{\mathrm{B}}}{I_{\mathrm{A}} + \dfrac{V_{\mathrm{B}}'' - V_{\mathrm{B}} - (V_{\mathrm{A}}'' - V_{\mathrm{A}})}{Z_{\mathrm{E}}}}$$

Substitute (5.23) and (5.24) to (5.10) to calculate $V_{\mathrm{sB}}$:

$$V_{\mathrm{sB}} = V_{\mathrm{B}} + Z_{\mathrm{B}} \left( -I_{\mathrm{A}} + \frac{V_{\mathrm{B}} - V_{\mathrm{A}}}{Z_{\mathrm{E}}} \right) \tag{5.25}$$

### 5.2.3. RESULT

Study in section 5.2.2 shows that the two bus system's model can be estimated using voltage phasors at two terminals and current phasor at one terminal of the line. In PSCAD simulation of the single circuit line test case, three phase instantaneous voltages $V_{\mathrm{A}}$ and $V_{\mathrm{B}}$ at two terminals of the monitored line and instantaneous current $I_{\mathrm{A}}$ at terminal A are measured and are imported to MATLAB. PSCAD data is then processed in Matlab and voltage and current phasors are estimated using algorithms mentioned in chapter 2. Figure 5.7 and Figure 5.8 are estimated voltage and current phasors. The red dots in these figures represent three different moments of the fault. The first moment is $t_1 = 0.5s$ when fault hasn't occurred yet. The second moment $t_2 = 1.05s$ is when line is

connected to ground but two circuit breakers are still closed. The last one $t_3 = 2.7s$ is when both circuit breakers are opened. Phasor values at these three moments are obtained and are used to rebuild the network model.

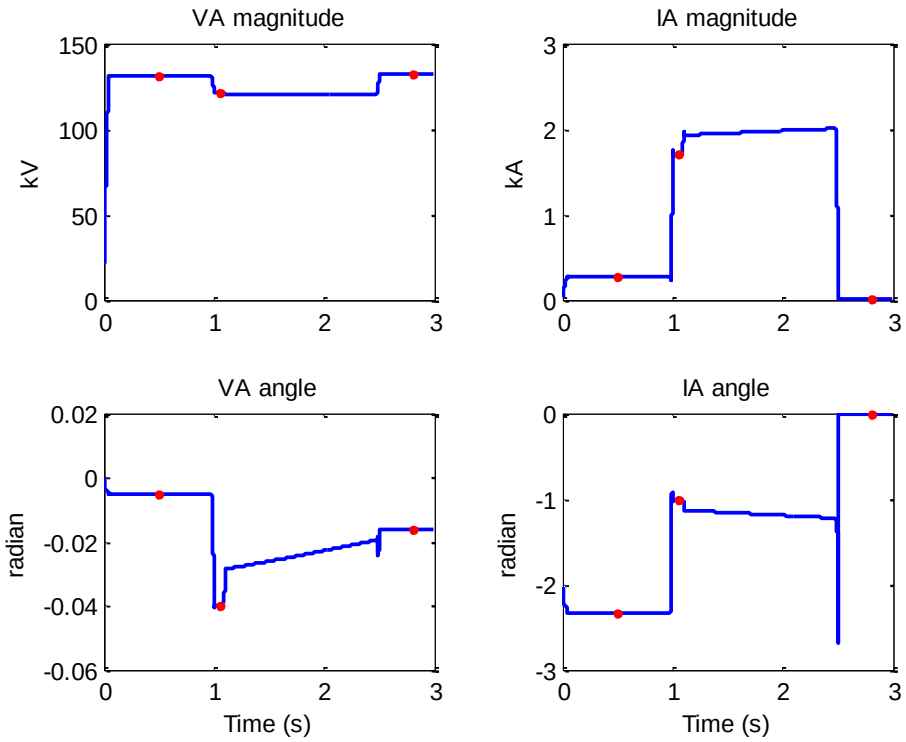


Figure 5.7: Voltage and current phasors at bus A

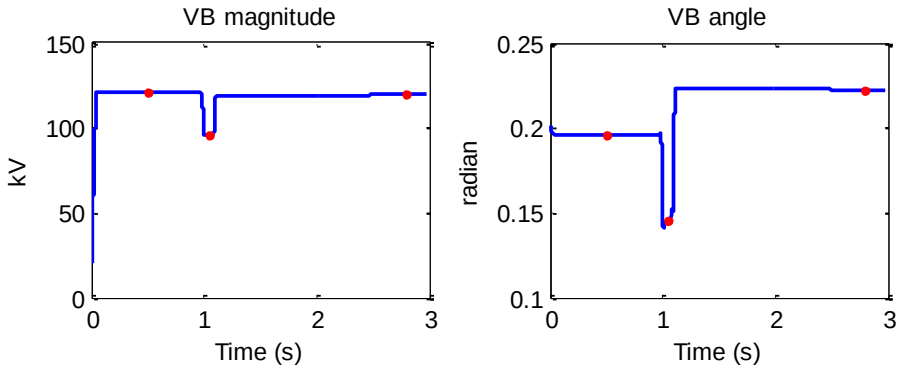


Figure 5.8: Voltage and current phasors at bus B

Using method discussed in section 5.2.2, the network model is calculated and is shown in Table 5.7:

Table 5.7: Single circuit line case model

| | |
|---|---|
| $V_{\mathrm{sA}}$ | 229.9732 ∠-1.3178° kV L-L |
| $Z_{\mathrm{A}}$ | 2.0300+5.9932i Ohm |
| $V_{\mathrm{sB}}$ | 206.9766 ∠13.6760° kV L-L |
| $Z_{\mathrm{B}}$ | 4.0546 +11.9833i Ohm |
| $Z_{\mathrm{E}}$ | 62.735+187.22i Ohm |

At moment $t_2$ we obtained value of voltage phasors at terminal A and B and current phasor at terminal A of the line in line. Using (4.48) (4.49) and (4.50), these values can be calculated from system's model described in Table 5.7. The calculated values are function of fault location and fault resistance:

$$V_i = f_i(x,\ R_F) \tag{5.26}$$

$$I_{jk} = g_{jk}(x,\ R_F) \tag{5.27}$$

Now the problem become solving equation with two variable $x$ and $R_F$:

$$\begin{bmatrix} f_{\mathrm{A}}(x,\ R_F) \\ f_B(x,\ R_F) \\ g_{\mathrm{AB}}(x,\ R_F) \end{bmatrix} - \begin{bmatrix} V_A \\ V_{\mathrm{B}} \\ I_{\mathrm{AB}} \end{bmatrix} = 0 \tag{5.28}$$

Equation (5.28) can be solved using non-linear least square method discussed in chapter 4. The solution is presented in Table 5.8.

Table 5.8: Single circuit line fault location result

| Faulted Resistance | Location of fault | Error in percentage of line length |
|---|---|---|
| 9.8082 Ohm | 59.97 % | 0.3 % |

## 5.3. DOUBLE CIRCUIT LINES CASE

Double circuit lines are common in power systems, basically due to the constraint in building new transmission line [8]. The double circuit lines are two three phase transmission circuits connecting one bus to another bus. In this section, a fault location method for double circuit lines is discussed. This can be considered an extension of the fault location technique using in single circuit line which has been presented in section 5.2. Basically, we need to decide which current and voltage measurement we do need to build the equivalent model of the network first. Then, method in chapter 4 will be applied to find the location of fault.

One issue with the double circuit lines or multiple circuit lines is the magnetic coupling effect. When one circuit is close to the other, its current will influence the other line's voltage. However, in this thesis, we only consider the case that mutual coupling effect is small and can be neglected.

### 5.3.1. SYSTEM DESCRIPTIONS

The pre-fault system is shown in Figure 5.9. Two terminals of the double circuit lines are name A and B. The system has voltage source $V_{\mathrm{sA}}$ and source impedance $Z_{\mathrm{A}}$ behind the terminal A, voltage source $V_{\mathrm{sB}}$ and source impedance $Z_{\mathrm{B}}$ behind terminal B of the line. Impedance $Z_{\mathrm{E}}$ connects terminal A and terminal B, represents the current flow

between two ends of the lines through the outside network. The system in Figure 5.9 is almost the same as the single circuit line case except the second line with impedance $Z_{\text{line2}}$ is added. Again, the line capacitance is assumed to be small and thus is not considered in this test case.

Component of system in Figure 5.9 are listed in Table 5.9.

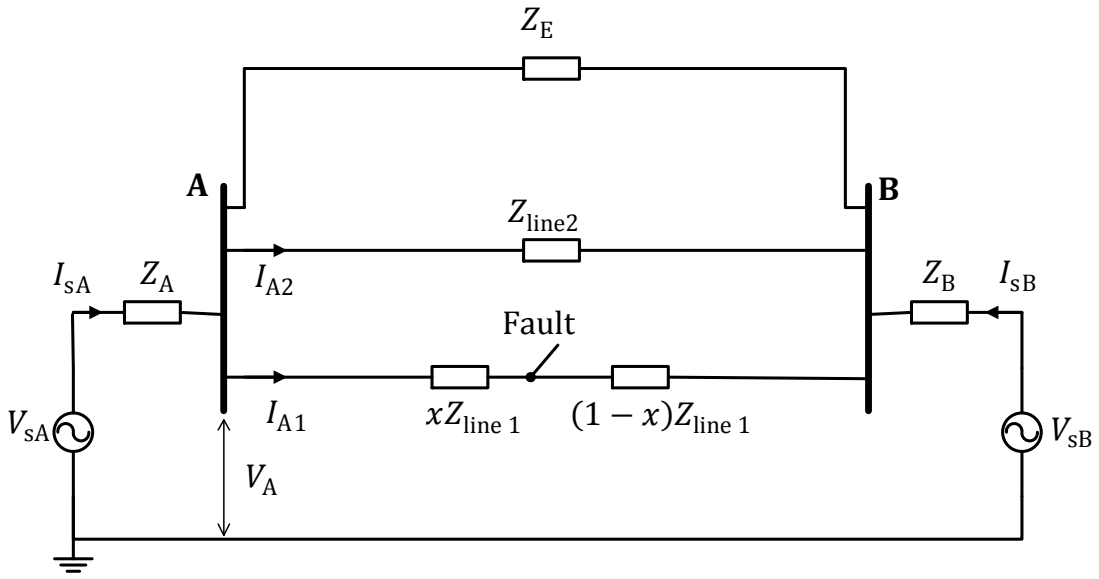


Figure 5.9: Double circuit lines test case

Table 5.9: Double circuit lines case

| | |
|---|---|
| $V_{\text{sA}}$ | 230∠0° kV L-L |
| $Z_{\text{A}}$ | 2+6i Ohm |
| $V_{\text{sB}}$ | 207∠15° kV L-L |
| $Z_{\text{B}}$ | 4+12i Ohm |
| $Z_{\text{E}}$ | 68+191i Ohm |
| $Z_{\text{line}}$ | 30.7 +93.1i Ohm |
| $Z_{\text{line2}}$ | 15.35 +46.5i Ohm |

A permanent three phase ground fault is simulated in PSCAD. The fault starts moment $t = 1$s in line 1 which has current $I_{A_1}$ denoted in Figure 5.9. The fault simulation also includes operation of two circuit breakers at terminal A and terminal B. The circuit breaker at terminal A trips $t = 1.1$s and the circuit breaker at bus B trips at $t = 2.5$s.

Because this test case has two lines being monitored, it is not necessary to collect data from both ends A and B. The following section 5.3.2 will show how to only measurement at one end to rebuild the network model.

### 5.3.2. SYSTEM MODELING

In this test case, we only have phasor measurements at bus A: $V_A, I_{A_1}$ and $I_{A_2}$. Assume that faults do not occur in two lines at the same time, the voltage at bus B can be estimated using voltage and currents measured at bus A and the parameters of the healthy line.

$$V_B = V_A - I_{A_2} Z_{\text{line2}} \tag{5.29}$$

(5.29) is always true as long as the line 2 is healthy. That means the estimation of voltage at bus B does not depend of status of circuit breakers on line 1.

$$V'_B = V'_A - I'_{A_2} Z_{\text{line2}} \tag{5.30}$$

$$V''_B = V''_A - I''_{A_2} Z_{\text{line2}} \tag{5.31}$$

Now the problem is to estimate model of the network with voltage and current measured at bus A and estimated voltage at bus B. The estimation is similar the process described in section 5.2.2. However, we don't need to find the impedance of extra link line $Z_E$ . Instead, the equivalent impedance $Z_{eq}$ which represents $Z_E$ in parallel with

$Z_{\text{line2}}$ will be estimated. Then the equivalent single circuit model is used to locate fault.

Using result from section 5.2.2, equations (5.29),(5.30) and (5.31), the equivalent model is:

$$\begin{cases} Z_{\text{A}} = \dfrac{c_1 b_2 - c_2 b_1}{a_1 b_2 - a_2 b_1} \\ V_{\text{sA}} = \dfrac{a_1 c_2 - a_2 c_1}{a_1 b_2 - a_2 b_1} \end{cases} \tag{5.32}$$

with $\text{a}_1 = \text{I}_{\text{A}}; \text{b}_1 = \frac{\text{I}_{\text{A}_2}}{\text{I}''_{\text{A}_2}} - 1; \text{c}_1 = \frac{\text{I}_{\text{A}_2}}{\text{I}''_{\text{A}_2}} \text{V}''_{\text{A}} - \text{V}_{\text{A}}; \text{a}_2 = (\text{I}'_{\text{A}} - \text{I}_{\text{A}}); \text{b}_2 = \frac{-\text{I}'_{\text{A}_2} + \text{I}_{\text{A}_2}}{\text{I}''_{\text{A}_2}}; \text{c}_2 =$

$\frac{-\text{I}'_{\text{A}_2} + \text{I}_{\text{A}_2}}{\text{I}''_{\text{A}_2}} \text{V}''_{\text{A}} - (\text{V}'_{\text{A}} - \text{V}_{\text{A}});$

$$Z_{\text{eq}} = \frac{c_1 b_2 - c_2 b_1}{a_1 b_2 - a_2 b_1} \times \frac{V''_{\text{A}} - V''_{\text{A}} + I''_{\text{A}_2} Z_{\text{line2}}}{\frac{a_1 c_2 - a_2 c_1}{a_1 b_2 - a_2 b_1} - V''_{\text{A}}} \tag{5.33}$$

$$Z_{\text{B}} = -\frac{V''_{\text{A}} - I''_{\text{A}_2} Z_{\text{line2}} - V_{\text{A}} + I_{\text{A}_2} Z_{\text{line2}}}{I_{\text{A}} + \frac{V''_{\text{A}} - I''_{\text{A}_2} Z_{\text{line2}} - V_{\text{A}} + I_{\text{A}_2} Z_{\text{line2}} - (V''_{\text{A}} - V_{\text{A}})}{Z_{\text{E}}}} \tag{5.34}$$

$$V_{\text{sB}} = V_{\text{A}} - I_{\text{A}_2} Z_{\text{line2}} + Z_{\text{B}} \left( -I_{\text{A}} - \frac{-I_{\text{A}_2} Z_{\text{line2}}}{Z_{\text{E}}} \right) \tag{5.35}$$

### 5.3.3. RESULT

Following the process described in single circuit line test case, voltage and current phasors are estimated. Figure 5.10 is voltage and current phasors at terminal A of the line. A set of phasor values at three moments are collected: pre-fault; during fault and when the faulted line is disconnected from the network. This set of data is used to calculate the model, shown in Table 5.10. The equivalent model obtained is a two bus network with an extra link line with impedance $Z_{\text{eq}}$. The value of $Z_{\text{eq}}$ is, however, not the same as the value of $Z_{\text{E}}$ in Figure 5.9 because of the second line with impedance $Z_{\text{line2}}$.

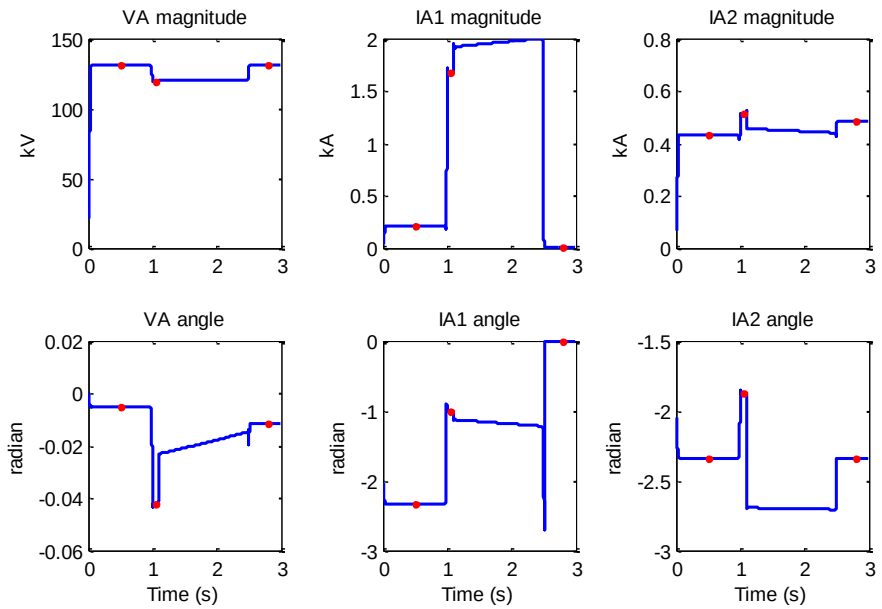


Figure 5.10: Voltage and current phasor at bus A

Table 5.10: Equivalent model of the double circuit lines case

| | |
|---|---|
| $V_{sA}$ | 229.97 ∠-2.1° kV L-L |
| $Z_A$ | 2.03 + 5.99i Ohm |
| $V_{sB}$ | 207∠12.81° kV L-L |
| $Z_B$ | 3.97 +11.98i Ohm |
| $Z_{eq}$ | 12.33 +37.34 Ohm |
| $Z_{line1}$ | 30.735 +93.251i Ohm |

Table 5.11: Single circuit line fault location result

| Faulted Resistance | Location of fault | Error in percentage of line length |
|---|---|---|
| 9.7498 Ohm | 60.03 % | 0.3 % |

Now, using the model shown in Table 5.10 to match the fault data at moment $t_2$, the fault location is found.

# CHAPTER 6

# CONCLUSION AND FUTURE WORK

## 6.1. CONCLUSION

The thesis develops a novel method for precise frequency measurement. The impact of difference between input signal's frequency and system's nominal frequency to the accuracy of classical frequency estimation method is analyzed. Mathematic expression of Discrete Fourier Transform at fundamental frequency shows that it is proportional to a sum of two vectors which have opposite phase angles and the error is negligible when one of the two vectors is close to zero, which is the case of nominal frequency input. By modifying the Discrete Fourier Transform calculation and properly selecting the linear combination of calculated terms at different frequency, the estimate is achieved precisely. Testing in MATLAB shows that proposed method can estimate the frequency accurately although additional filter is not applied. The maximum error in a wide range of frequency is smaller in comparison with classical method. Testing the proposed method with input signal that has varying frequency also shows accurate result. This ability to track time varying frequency is important when monitored power systems are transient. Another advantage of this algorithm is the ability to reduce report delay since no additional filter is required to remove ripple in estimated frequency. This feature is useful when measurement is used in protection application which requires fast response.

Voltage and current phasors are used to locate fault in power network. The fault

location technique involves the calculation of network impedance matrix as a function of fault location and fault resistance. Then using iteration process, variables represent fault location and fault resistance are adjusted to match the calculated voltage and current and the voltage and current measured at various location in the network during fault. This approach is applied to three example cases: six bus network, single circuit line and double circuit lines. All three example cases are simulated in PSCAD and waveforms are imported to MATLAB to validate the fault location technique. In the six bus network, using the provided network model, the location of fault is found with small error. For the single circuit line and double circuit lines example, the thesis presents method to acquire system's model using limited voltage and current measurements. For both cases, equivalent two bus system models are obtained and then are used in the iteration process. The fault location is found accurately in each case.

## 6.2. FUTURE WORK

Since phasor is the term defined to represent ideal sinusoidal function of time, one issue of phasor estimation or frequency estimation techniques is the reliability of its estimate when input signal is transient. The frequency estimation algorithm presented is accurate for the case of ideal sinusoidal input signal and even for the case of signal with time varying frequency which is relatively slow in comparison with system's nominal frequency. However, method to monitoring bad data is needed to ensure the reliability of its result. Additional testing with different transient input signals is necessary to verify that the algorithms work in all cases.

The fault location algorithm is shown to be accurate for the three test cases. Equivalent models of the single circuit line and the double circuit lines examples but for the general

case, network model needs to be provided. Investigation into the network modeling and related issues such as minimum placement of PMU devices for fault location purpose is necessary. The fault location method also assumes fault inception is detected correctly. Equivalent models of the single circuit line and the double circuit lines examples are obtained assuming pre-fault and during fault data are selected correctly. However, the evolution of a fault in power system could be complicated considers the operation of protection devices. Reliable techniques that can identify each stage of the fault will be useful. In addition, from practical perspective, related issues such as implementation of algorithms into hardware optimize cost and performance, communication problem, etc. is important to bring the presented method into practice.

The scope of this thesis is limited to balanced three phase fault location but it is promising to expand the approach presented in this thesis to other fault types. For example, un-balanced short circuit fault can be represented by an injection of fault current into the positive sequence circuit model. Now, the fault location problem becomes similar to the balanced fault case with unknown variables are fault location and fault current.

# REFERENCES


[1] U.S.-Canada Power System Outage Task Force, “Final Report on the August 14, 2003 Blackout in the United States and Canada: Causes and Recommendations,” Technical Report, April 2004.

[2] NERC Steering Group, “Technical Analysis of the August 14, 2003, Blackout: What Happened, Why, and What Did We Learn?,” North American Electric Reliability Council, Princeton, New Jersey, July 2004.

[3] “Key Facts about the Electric Power Industry,” Edison Electric Institute, www.eei.org, August 2006.

[4] J. D. Glover, M. S. Sarma, T. J. Overbye, “Power System Analysis and Design,” Australia Toronto, Thomson, 2008.

[5] “Synchrophasor Technology Roadmap,” North American Synchrophasor Initiative, March 2009.

[6] J. L. Blackburn, “Protective Relaying,” Dekker, New York, 1997.

[7] Chunchun Xu, ``High Accuracy Real-time GPS Synchronized Frequency Measurement Device for Wide-area Power Grid Monitoring," Doctoral Desertation, Virginia Tech, Virginia, Feb 2006.

[8] M. M. Saha, J. Izykowski, E. Rosolowski, “Fault Location on Power Networks,” Springer, 2009

[9] "IEEE Standard for Synchrophasor Measurements for Power Systems,” IEEE Std C37.118.1-2011 (Revision of IEEE Std C37.118-2005) , vol., no., pp.1-61, Dec. 28 2011

[10] Adly A. Girgis and Fredric M. Ham, “A new FFT-based digital frequency relay for load shedding,” in IEEE Transactions on Power Apparatus and System, Vol. PAS-101, No.2 Feb 1982.

[11] Jun-Zhe Y. and Chih-Wen L., "A precise calculation of power system frequency and phasor," IEEE Transactions on Power Delivery, Vol. 15, No. 2 , April 2000, pp 494–499

[12] Dash, P.K., Panda, S.K., Mishra, B., and Swain, D.P., "Fast estimation of volt-age and current phasors in power networks using an adaptive neural network," IEEE Transactions on Power Systems, Vol. 12, No. 4 , November 1997, pp 1494–1499

[13] Girgis, A.A. and Brown, R.G., "Application of Kalman filtering in computer relaying," IEEE Transactions on Power Apparatus and Systems, Vol. PAS-100, July 1981.

[14] Chi-Kong W., Ieng-Tak L., Chu-San L., Jing-Tao W., and Ying-Duo H., "A novel algorithm for phasor calculation based on wavelet analysis," Power Engineering Society Summer Meeting, 2003, IEEE, Vol. 3, 15–19 July 2001 pp. 1500–1503.

[15] A. Phadke, A. Stankovic, J. Thorp, and M. Pai, "Synchronized Phasor Measurements and Their Applications," Springer, 2008.

[16] "Real-Time Application of Synchrophasors for Improving Reliability," North American Electric Reliability Corporation (NERC), Tech. Rep., Oct. 2010.

[17] L.V. Bewley, "Travelling Waves on Transmission Systems," John Wiley & Sons, Inc., New York, 1963.

[18] J, T. Abrams, "Voltage-only Fault Location on Power Transmission System via Digital Signal Processing Techniques," Master Thesis, University of South Carolina, South Carolina, 2006.

[19] H.E. Brown, "Solution of Large Networks by Matrix Methods," Wiley, New York, 1985.